Kralovics R, Passamonti F, Buser AS, Teo SS, Tiedt R, Passweg JR *et al.* (2005). A gain-of-function mutation of JAK2 in myeloproliferative disorders. *N Engl J Med* **352**: 1779–1790.

Kubonishi I, Miyoshi I. (1983). Establishment of a Ph1 chromosome-positive cell line from chronic myelogenous leukemia in blast crisis. *Int J Cell Cloning* **1**: 105–117.

Kwong YL, Wong KF, Chan V, Chan CH. (1996). Persistence of AML1 rearrangement in peripheral blood cells in t(8;21). *Cancer Genet Cytogenet* **88**: 151–154.

Ley TJ, Mardis ER, Ding L, Fulton B, McLellan MD, Chen K *et al.* (2008). DNA sequencing of a cytogenetically normal acute myeloid leukaemia genome. *Nature* **456**: 66–72.

Miyamoto T, Nagafuji K, Akashi K, Harada M, Kyo T, Akashi T *et al.* (1996). Persistence of multipotent progenitors expressing AML1/ETO transcripts in long-term remission patients with t(8;21) acute myelogenous leukemia. *Blood* **87**: 4789–4796.

Miyamoto T, Weissman IL, Akashi K. (2000). AML1/ETO-expressing nonleukemic stem cells in acute myelogenous leukemia with 8;21 chromosomal translocation. *Proc Natl Acad Sci USA* **97**: 7521–7526.

Nimer SD, Moore MA. (2004). Effects of the leukemia-associated AML1-ETO protein on hematopoietic stem and progenitor cells. *Oncogene* **23**: 4249–4254.

Okano M, Bell DW, Haber DA, Li E. (1999). DNA methyltransferases Dnmt3a and Dnmt3b are essential for *de novo* methylation and mammalian development. *Cell* **99**: 247–257.

Onishi M, Kinoshita S, Morikawa Y, Shibuya A, Phillips J, Lanier LL *et al.* (1996). Applications of retrovirus-mediated expression cloning. *Exp Hematol* **24**: 324–329.

Patil N, Berno AJ, Hinds DA, Barrett WA, Doshi JM, Hacker CR *et al.* (2001). Blocks of limited haplotype diversity revealed by high-resolution scanning of human chromosome 21. *Science* **294**: 1719–1723.

Pikman Y, Lee BH, Mercher T, McDowell E, Ebert BL, Gozo M *et al.* (2006). MPLW515L is a novel somatic activating mutation in myelofibrosis with myeloid metaplasia. *PLoS Med* **3**: e270.

Russell SM, Tayebi N, Nakajima H, Riedy MC, Roberts JL, Aman MJ *et al.* (1995). Mutation of Jak3 in a patient with SCID: essential role of Jak3 in lymphoid development. *Science* **270**: 797–800.

Sato T, Toki T, Kanezaki R, Xu G, Terui K, Kanegane H *et al.* (2008). Functional analysis of JAK3 mutations in transient myeloproliferative disorder and acute megakaryoblastic leukaemia accompanying Down syndrome. *Br J Haematol* **141**: 681–688.

Schlenk RF, Dohner K, Krauter J, Frohling S, Corbacioglu A, Bullinger L *et al.* (2008). Mutations and treatment outcome in cytogenetically normal acute myeloid leukemia. *N Engl J Med* **358**: 1909–1918.

Schwonzen M, Diehl V, Dellanna M, Staib P. (2007). Immunophenotyping of surface antigens in acute myeloid leukemia by flow cytometry after red blood cell lysis. *Leuk Res* **31**: 113–116.

Shimada A, Taki T, Tabuchi K, Tawa A, Horibe K, Tsuchida M *et al.* (2006). KIT mutations, and not FLT3 internal tandem duplication, are strongly associated with a poor prognosis in pediatric acute myeloid leukemia with t(8;21): a study of the Japanese Childhood AML Cooperative Study Group. *Blood* **107**: 1806–1809.

Sjoblom T, Jones S, Wood LD, Parsons DW, Lin J, Barber TD *et al.* (2006). The consensus coding sequences of human breast and colorectal cancers. *Science* **314**: 268–274.

Suetake I, Miyazaki J, Murakami C, Takeshima H, Tajima S. (2003). Distinct enzymatic properties of recombinant mouse DNA methyltransferases Dnmt3a and Dnmt3b. *J Biochem* **133**: 737–744.

Tallman MS, Altman JK. (2008). Curative strategies in acute promyelocytic leukemia. *Hematol Am Soc Hematol Educ Program* **2008**: 391–399.

Walters DK, Mercher T, Gu TL, O'Hare T, Tyner JW, Loriaux M *et al.* (2006). Activating alleles of JAK3 in acute megakaryoblastic leukemia. *Cancer Cell* **10**: 65–75.

Wheeler DA, Srinivasan M, Egholm M, Shen Y, Chen L, McGuire A *et al.* (2008). The complete genome of an individual by massively parallel DNA sequencing. *Nature* **452**: 872–876.

Wong S, Witte ON. (2001). Modeling Philadelphia chromosome positive leukemias. *Oncogene* **20**: 5644–5659.

Yamamoto Y, Kiyoi H, Nakano Y, Suzuki R, Kodera Y, Miyawaki S *et al.* (2001). Activating mutation of D835 within the activation loop of FLT3 in human hematologic malignancies. *Blood* **97**: 2434–2439.

Supplementary Information accompanies the paper on the Oncogene website (http://www.nature.com/onc)

Cell Stem Cell
Article

TIM-3 Is a Promising Target to Selectively Kill Acute Myeloid Leukemia Stem Cells

Yoshikane Kikushige,[1] Takahiro Shima,[1] Shin-ichiro Takayanagi,[2] Shingo Urata,[1] Toshihiro Miyamoto,[1] Hiromi Iwasaki,[1] Katsuto Takenaka,[1] Takanori Teshima,[1] Toshiyuki Tanaka,[3] Yoshimasa Inagaki,[2] and Koichi Akashi[1,*]
[1]Department of Medicine and Biosystemic Sciences, Kyushu University Graduate School of Medicine, Fukuoka 812-8582, Japan
[2]Innovative Drug Research Laboratories Kyowa Hakko Kirin Co., Ltd., Tokyo 194-8538, Japan
[3]School of Pharmacy, Hyogo University of Health Sciences, Kobe 650-8530, Japan
*Correspondence: akashi@med.kyushu-u.ac.jp
DOI 10.1016/j.stem.2010.11.014

SUMMARY

Acute myeloid leukemia (AML) originates from self-renewing leukemic stem cells (LSCs), an ultimate therapeutic target for AML. Here we identified T cell immunoglobulin mucin-3 (TIM-3) as a surface molecule expressed on LSCs in most types of AML except for acute promyelocytic leukemia, but not on normal hematopoietic stem cells (HSCs). TIM-3$^+$ but not TIM-3$^-$ AML cells reconstituted human AML in immunodeficient mice, suggesting that the TIM-3$^+$ population contains most, if not all, of functional LSCs. We established an anti-human TIM-3 mouse IgG2a antibody having complement-dependent and antibody-dependent cellular cytotoxic activities. This antibody did not harm reconstitution of normal human HSCs, but blocked engraftment of AML after xenotransplantation. Furthermore, when it is administered into mice grafted with human AML, this treatment dramatically diminished their leukemic burden and eliminated LSCs capable of reconstituting human AML in secondary recipients. These data suggest that TIM-3 is one of the promising targets to eradicate AML LSCs.

INTRODUCTION

Acute myeloid leukemia (AML) is a clonal malignant disorder derived from a small number of leukemic stem cells (LSCs). LSCs self renew and generate leukemic progenitors that actively divide to produce a large number of immature clonogenic leukemic blasts (Bonnet and Dick, 1997; Hope et al., 2004; Lapidot et al., 1994). This hierarchical stem cell-progenitor-mature cell relationships in AML appears to simulate normal hematopoiesis that originates from hematopoietic stem cells (HSCs) with self-renewal activity. We have shown that like normal HSCs, AML LSCs are quiescent in vivo and appear to reside at the endosteal "osteoblastic" niche in the bone marrow based on our analysis in a xenograft model (Ishikawa et al., 2007). AML LSCs are resistant to chemotherapeutic reagents that usually target cycling malignant cells. In the majority (~90%) of AML patients, the conventional chemotherapies can diminish the leukemic clones to achieve remission. However, ~60% of such remission patients still relapse, and the recurrence of AML in these patients should originate from LSCs that survive the intensive chemotherapies. Therefore, the LSC should be the ultimate cellular target to cure human AML.

To eradicate the AML LSC without killing normal HSCs, it is critical to isolate a molecule that is expressed or functions specifically at the AML LSC stage (Krause and Van Etten, 2007). It has been shown that the AML LSCs mainly reside within the CD34$^+$CD38$^-$ fraction of leukemic cells and can reconstitute human AML in immunodeficient mice (Lapidot et al., 1994), although recent studies have suggested that LSCs can exist also in CD34$^+$CD38$^+$ (Taussig et al., 2008) or CD34$^-$ blastic fractions at least in some types of AML (Martelli et al., 2010; Taussig et al., 2010). Normal HSCs with long-term reconstitution activity also have the CD34$^+$CD38$^-$ phenotype (Bhatia et al., 1997; Ishikawa et al., 2005). However, the expression pattern of other surface molecules in the CD34$^+$CD38$^-$ fraction of AML cells is different from that of normal controls. For example, CD34$^+$CD38$^-$ AML cells possess many phenotypic characteristics analogous to normal granulocyte/macrophage progenitors (GMPs) (Yoshimoto et al., 2009). Previous studies have reported molecules preferentially expressed in AML cells. Such molecules include CLL-1 (van Rhenen et al., 2007), CD25, CD32 (Saito et al., 2010), CD33 (Florian et al., 2006; Hauswirth et al., 2007), CD44 (Florian et al., 2006; Jin et al., 2006), CD47 (Jaiswal et al., 2009; Majeti et al., 2009), CD96 (Hosen et al., 2007), and CD123 (Jin et al., 2009; Yalcintepe et al., 2006). However, in our hands, some of these molecules are expressed in LSCs at a level insufficient for clear distinction, are expressed also in normal HSCs at a considerable level, or are found only in a fraction of AML cases. It is therefore critical to isolate ideal targets for AML LSCs with sufficient specificity and sensitivity.

Here we report a new surface molecule that might be useful to eradicate AML LSCs leaving normal HSC intact. We performed differential transcriptional profiling of AML LSCs and HSCs and extracted the T cell immunoglobulin mucin-3 (TIM-3) as a promising AML LSC-specific target surface molecule. TIM-3 is originally found as a surface molecule expressed in CD4$^+$ Th1 lymphocytes in mouse hematopoiesis and is an important regulator of Th1 cell immunity and tolerance induction (Monney et al., 2002; Sabatos et al., 2003; Sánchez-Fueyo et al., 2003). Murine TIM-3 is also expressed in CD11b$^+$ macrophages and CD11c$^+$ dendritic cells and recognizes apoptotic cells' phosphatidylserine through its IgV domain to mediate phagocytosis (Nakayama et al., 2009).

We found that human TIM-3 was expressed in the vast majority of CD34$^+$CD38$^-$ LSCs and CD34$^+$CD38$^+$ leukemic progenitors in AML of most FAB types, except for acute

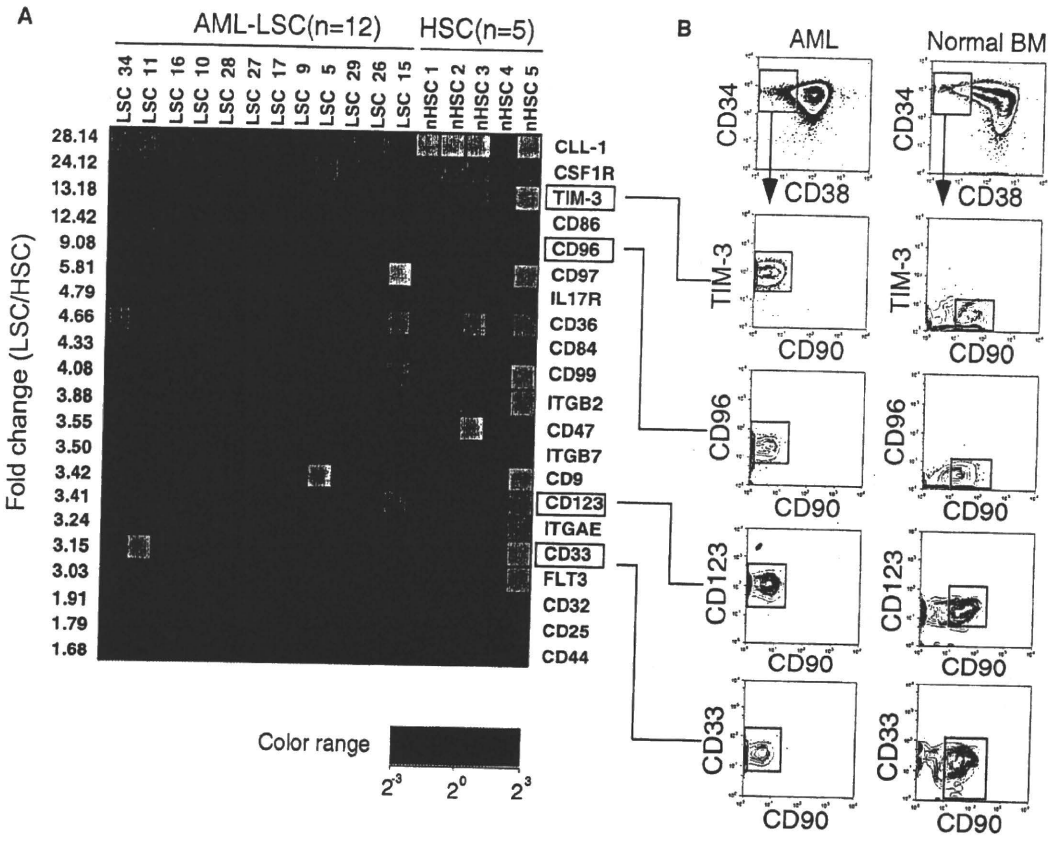

Figure 1. The Expression of LSC-Specific Surface Molecules in AML

The $CD34^+CD38^-$ adult bone marrow HSCs and $CD34^+CD38^-$ AML LSCs were purified and tested for their surface molecule expression.

(A) Results of cDNA microarray analysis of HSCs and AML LSCs. Representative genes coding surface molecules that are expressed highly in AML LSCs are shown. TIM-3 is expressed specifically in LSCs at high levels in the majority of AML patients. Patient numbers correspond to those in Table S1.

(B) The expression of representative surface proteins in HSCs and AML LSCs on FACS.

promyelocytic leukemia (M3). TIM-3 was not expressed in $CD34^+CD38^-$ normal HSCs or the vast majority of $CD34^+$ $CD38^+$ normal progenitors. Administration of anti-human TIM-3 mouse antibodies with a complement-dependent cytotoxicity (CDC) and an antibody-dependent cellular cytotoxicity (ADCC) selectively inhibited engraftment and development of human AML in xenograft models. Our data strongly suggest that the use of TIM-3 to target AML LSCs is a promising approach for the improvement of leukemia therapy.

RESULTS

TIM-3 Is Expressed in the $CD34^+CD38^-$ Fraction of AML Patients' Bone Marrow Cells

In most types of AML, LSCs are concentrated in the $CD34^+$ $CD38^-$ fraction of AML cells (Ishikawa et al., 2007; Lapidot et al., 1994), whose phenotype is common to normal adult HSCs. Patients' characteristics are shown in Table S1 available online. To search for the AML LSC-specific molecules, 10,000 each of purified $CD34^+CD38^-$ AML cells and $CD34^+CD38^-$ normal HSCs were subjected to cDNA microarray analysis. We extracted 256 genes with >4-fold change between normal HSCs and $CD34^+CD38^-$ AML cells and then selected 197 differentially expressed genes with <0.01 of a cut-off p value (Table S2). Genes coding surface molecules that are expressed highly in $CD34^+CD38^-$ AML cells were selected for this study. Figure 1A shows the mRNA levels of candidate LSC-specific surface molecules in purified $CD34^+CD38^-$ AML cells and normal HSCs. The molecules expressed in $CD34^+CD38^-$ AML cells at levels >8-fold higher as compared to normal HSCs included TIM-3 and previously identified LSC-specific molecules such as CLL-1 (van Rhenen et al., 2007), CSF1R (Aikawa et al., 2010), and CD96 (Figure 1A; Hosen et al., 2007). As shown in Figure 1B, TIM-3 protein was highly expressed in $CD34^+CD38^-$ AML cells but not in normal HSCs. We focused on TIM-3 not only because it is expressed specifically in $CD34^+CD38^-$ AML cells at high levels, but also because it is expressed in the majority of patients with most AML types.

We evaluated the TIM-3 protein expression on cell surface of AML cells by FACS analysis. As shown in Figure 2, the vast majority of the $CD34^+CD38^-$ LSCs as well as $CD34^+CD38^+$ progenitor fractions in AML M0, M1, M2, and M4 types expressed TIM-3 at a high level in virtually all cases studied. In AML M5, M6, and M7, a considerable fraction of $CD34^+CD38^-$ cells

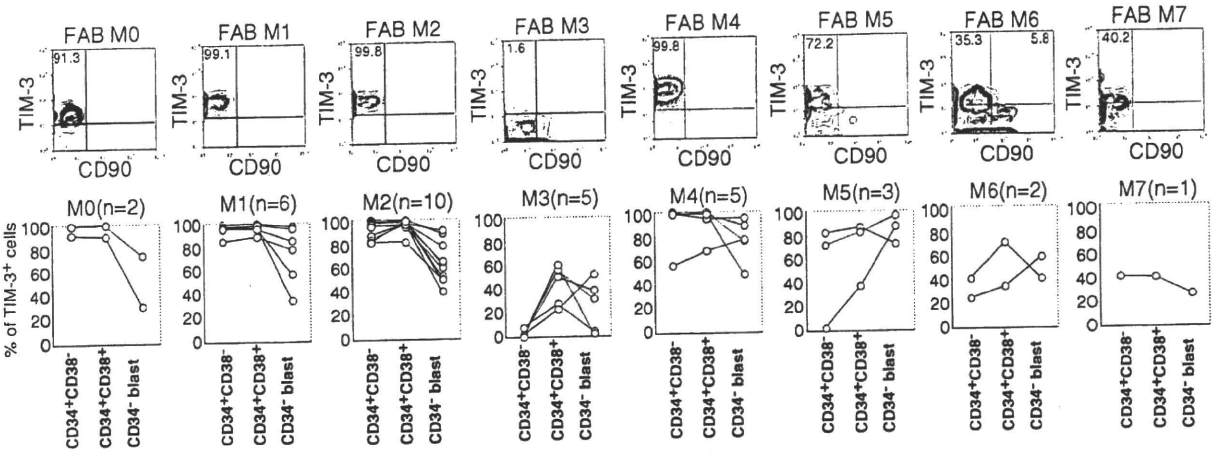

Figure 2. The Expression of TIM-3 in Stem and Progenitor Populations of AML of Each FAB Type
Expression of TIM-3 in each FAB type of AML. The representative expression pattern of TIM-3 in the $CD34^+CD38^-$ LSC fraction (top) and distribution of TIM-3 in $CD34^+CD38^-$ LSCs, $CD34^+CD38^+$ leukemic progenitors, and $CD34^-$ leukemic blasts (bottom) are shown.

expressed TIM-3. TIM-3 was, however, not expressed in the $CD34^+CD38^-$ population in all five M3 cases tested. In general, TIM-3 was expressed in both $CD34^+CD38^-$ LSCs and $CD34^+CD38^+$ leukemic progenitor fractions, but its expression tended to decline at the $CD34^-$ leukemic blast stage (Figure 2, bottom).

The TIM-3-Expressing of AML Fraction Contains the Vast Majority of Functional LSCs in a Xenograft Model

Recent studies have suggested that at least in some AML cases, LSCs that are capable of initiating human AML in xenograft models reside not only within the $CD34^+CD38^-$ fraction but also outside of this population including $CD34^+CD38^+$ (Taussig et al., 2008) or $CD34^-$ (Martelli et al., 2010; Taussig et al., 2010) AML cells. To evaluate whether functional AML LSCs express TIM-3, 10^6 cells of human $TIM\text{-}3^+$ and $TIM\text{-}3^-$ AML populations were transplanted into sublethally irradiated immunodeficient mice. We used NOD.Cg-*Rag1*^{tm1Mom} *Il2rg*^{tm1Wjl}/SzJ (NRG) mice for the xenogeneic transplantation experiments, by which higher chimerism of human hematopoietic cells was observed in xenotransplantation assays (Pearson et al., 2008). Recipients transplanted with $TIM\text{-}3^+$ and $TIM\text{-}3^-$ AML cells were sacrificed 8–10 weeks after transplantation. As shown in Figure 3, human $CD45^+CD33^+$ AML cells were

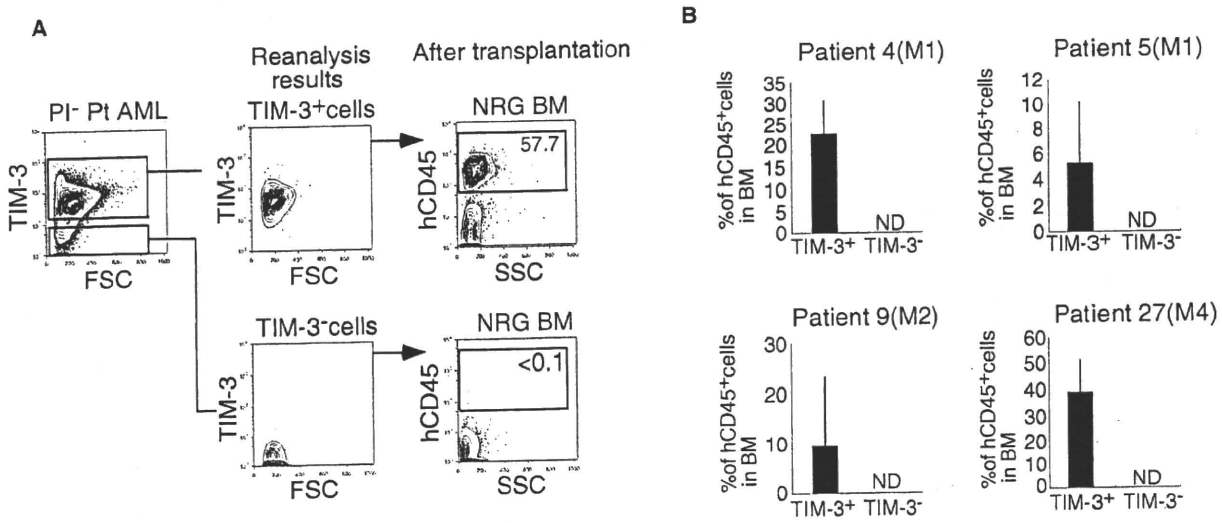

Figure 3. The $TIM\text{-}3^+$ AML Population Contains the Vast Majority of Functional LSC Activity
(A) A representative analysis of xenotransplantation of purified $TIM\text{-}3^+$ or $TIM\text{-}3^-$ AML cells from patient 27 into NRG mice. Only $TIM\text{-}3^+$ cells reconstitute $hCD45^+$ AML cells after transplantation.
(B) Summarized data of four independent experiments. Only $TIM\text{-}3^+$ (not $TIM\text{-}3^-$) AML cells reconstituted human AML cells in xenotransplantation experiments in all experiments, suggesting that most functional LSCs reside in the $TIM\text{-}3^+$ AML fraction.

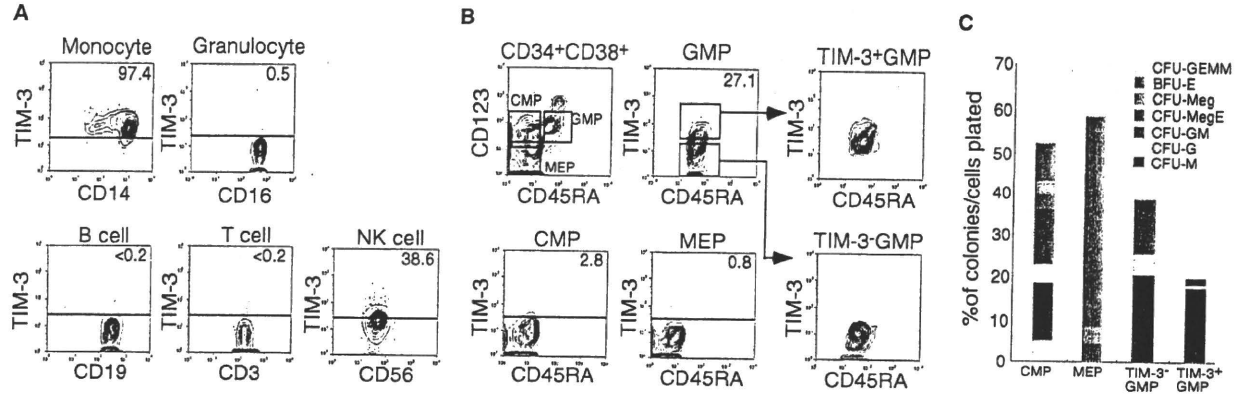

Figure 4. TIM-3 Is Expressed in Monocytes and Their Progenitors in Normal Hematopoiesis
(A) TIM-3 expression in normal mature blood cells.
(B) TIM-3 expression in normal hematopoietic progenitors. A fraction of GMPs but not other myeloid progenitors express TIM-3.
(C) Results of clonogenic assays of myelo-erythroid progenitors including single TIM-3$^+$ GMPs out of five independent experiments. The vast majority of TIM-3$^+$ GMPs gave rise to macrophage colonies (CFU-M).

reconstituted only in mice transplanted with TIM-3$^+$ AML cells, whereas TIM-3$^-$ AML cells failed to reconstitution in all four AML cases tested (Figure 3B). Thus, all 23 mice injected with TIM-3$^+$ AML cells reconstituted human AML, whereas 11 mice injected with TIM-3$^-$ AML never developed human AMLs after transplantation. These results strongly suggest that LSCs exclusively reside within the TIM-3$^+$ fraction in human AML at least in these patients.

TIM-3 Is Not Expressed in Normal Adult HSCs, and Its Expression Begins after Cells Are Committed to the Monocyte Lineage

Murine TIM-3 is expressed in a fraction of Th1 cells, monocytes, dendritic cells, and mast cells (Anderson et al., 2007; Monney et al., 2002; Nakae et al., 2007). The expression of human TIM-3 protein in normal steady-state human hematopoiesis is shown in Figures 4A. In periphery, TIM-3 was expressed in monocytes and a fraction of NK cells, but not in granulocytes, T cells, or B cells (Figure 4A). In the bone marrow, TIM-3 was not expressed in normal HSCs (Figure 1) or the vast majority of the CD34$^+$CD38$^+$ progenitor population. Within the CD34$^+$CD38$^+$ fraction, TIM-3 was expressed only in a fraction of GMPs at a low level, but not in common myeloid progenitors (CMPs), megakaryocyte/erythrocyte progenitors (MEPs) (Figure 4B), or common lymphoid progenitors (CLPs) (not shown). In clonogenic colony-forming unit (CFU) assays, the vast majority of purified TIM-3$^+$ GMPs gave rise to CFU-M, whereas colonies derived from TIM-3$^-$ GMP contained CFU-GM as well as CFU-G and CFU-M (Figure 4C). These data strongly suggest that TIM-3 up-regulation mainly occurs in concert with the monocyte lineage commitment at the GMP stage in normal hematopoiesis.

Anti-Human TIM-3 Antibodies Did Not Impair Development of Normal Hematopoiesis

To selectively eliminate TIM-3-expressing AML LSCs in vivo, we developed a monoclonal antibody against TIM-3 that has an efficient interaction with cellular Fc receptors on innate immune effector cells. It has become clear that the ADCC activity is one of the most important factors to eliminate target cells in antibody therapies (Nimmerjahn and Ravetch, 2007). A TIM-3 monoclonal antibody (IgG2b) was obtained by immunizing Balb/c mice with L929 cells stably expressing human TIM-3 and soluble TIM-3 protein. The variable portion of the VH regions of the cloned hybridoma that recognize TIM-3 were then grafted onto IgG2a Fc regions, because IgG2a subclass is most efficient to induce ADCC activity in mice (Nimmerjahn and Ravetch, 2005; Uchida et al., 2004). The established clone, ATIK2a, possessed CDC activities in EoL-1 and L929 cells transfected with TIM-3 (Figure 5A), as well as Kasumi-3, an AML cell line that spontaneously expresses TIM-3 (not shown). Importantly, ATIK2a displayed strong ADCC activity against TIM-3-expressing EoL-1 and L929 cells in vitro (Figure 5B).

We first tested the effect of ATIK2a treatment on reconstitution of normal HSCs in a xenograft model. The major effectors in ADCC reaction are NK cells. Because NRG mice do not have NK cells because of γc mutation (Pearson et al., 2008), we used NOD-SCID mice for this experiment to potentiate ADCC activity of ATIK2a antibodies. NOD-SCID mice were sublethally irradiated and were transplanted with 10^5 CD34$^+$ adult human bone marrow cells. 15 μg of ATIK2a was intraperitoneally injected to mice 12 hr after transplantation, which was followed by further injections of 15 μg of ATIK2a once a week until mice were sacrificed at 12 weeks after transplantation. Injection of ATIK2a did not affect reconstitution of normal hematopoiesis: The percentage of human cells were equal (~1%), and human B and myeloid cells were normally reconstituted irrespective of ATIK2a treatment in three independent experiments (not shown). We also tested the effect of this ATIK2a treatment in NOD-SCID mice transplanted with 10^5 CD34$^+$ cord blood cells. Cord blood cells have potent reconstitution activity in NOD-SCID mice, and percentage of hCD45$^+$ human cells reached ~50% after transplantation (Figure 5C). Again, the chimerism of human cells was equal, and CD19$^+$ B cells and CD33$^+$ myeloid cells were reconstituted irrespective of ATIK2a treatment (Figure 5C, left). In mice injected with ATIK2a, however, human TIM-3$^+$ monocytes were removed (Figure 5C, right). These data suggest that

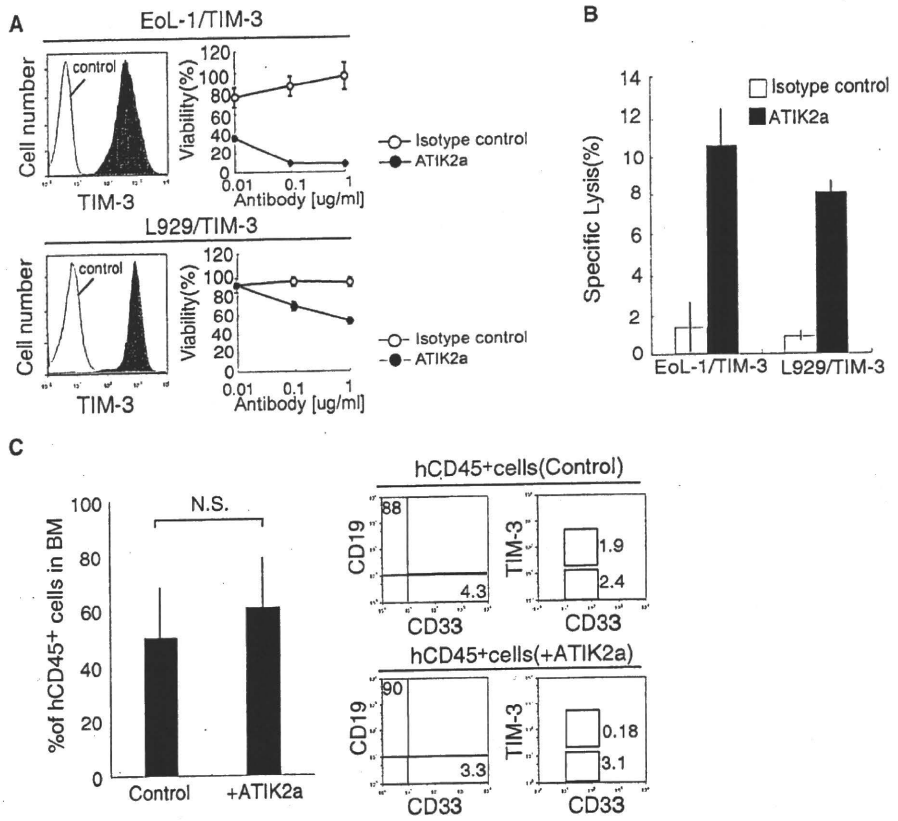

Figure 5. ATIK2a, a New Monoclonal Antibody against TIM-3, Has CDC and ADCC Activities and Does Not Harm Normal Hematopoietic Reconstitution

(A) CDC assays to evaluating the killing effect of ATIK2a antibodies on EoL-1 and L929 cell lines with enforced expression of human TIM-3.

(B) ADCC activities of ATIK2a on TIM-3-expressing EoL-1 and L929 cell lines.

(C) The effect of ATIK2a treatment on human hematopoietic reconstitution in NOD-SCID mice transplanted with 10^5 $CD34^+$ human cord blood cells. 15 μg of ATIK2a was intraperitoneally injected to mice 12 hr after transplantation, which was followed by further injections of 15 μg of ATIK2a once a week until mice were sacrificed at 12 weeks after transplantation. In this experiment, percentages of human cells in 10 each of mouse groups treated with control or ATIK2a antibodies were equivalent at 12 weeks after transplantation.

targeting TIM-3 does not affect development of normal hematopoiesis but remove TIM-3-expressing monocytes.

Anti-Human TIM-3 Antibodies Effectively Blocked Development of AML LSCs but Not that of Normal HSCs

We then tried to test the effect of ATIK2a in AML LSCs. We transplanted 10^6 bone marrow cells of AML patients (patients 6, 9, 15, 18, and 26) into NOD-SCID mice. The bone marrow of patients 6, 9, 15, and 26 were completely occupied with AML clones, and normal HSCs were not seen on FACS. Samples of each patient were transplanted into six mice, and three mice each were treated with 15 μg of ATIK2a or control IgG 12 hr after transplantation and with the same dose of antibodies once a week (Figure 6A). Mice were sacrificed 16 weeks after xenotransplantation. As shown in Figure 6B, the chimerism of AML cells were low in the NOD-SCID xenotransplant system. Nonetheless, ATIK2a injection significantly blocked AML reconstitution in these mice. In all of these patients, mice injected with control IgG showed reconstitution of $CD34^+TIM\text{-}3^+$ cells that contained primitive AML stem or progenitors as well as $CD33^+$ AML blasts (Figure 6B). In contrast, in mice treated with ATIK2a, the leukemic clone was barely detectable, and did not contain detectable numbers of $CD34^+$ cells (not shown), displaying significantly lower chimerisms as compared to control mice in all four independent experiments (Figure 6C).

The bone marrow of patient 18 possessed a small fraction of $CD34^+CD38^-CD90^+TIM\text{-}3^-$ cells that was phenotypically normal HSCs, in addition to the major fraction of $CD34^+CD38^-CD90^-TIM\text{-}3^+$ AML LSCs (Figure 6D). Interestingly, in mice transplanted with the bone marrow from this patient, ATIK2a injection induced reconstitution of normal myeloid and B cells, whereas control mice developed AML. These data strongly suggest that the ATIK2a treatment selectively inhibited development of human AML, presumably by targeting LSCs, instead allowing normal HSCs to reconstitute human hematopoiesis in vivo.

TIM-3 Targets Leukemic Stem Cells

In testing the inhibitory effect of ATIK2a on established human AML in a xenotransplant system, we used the NRG mice to increase engraftment efficiency of human AML cells. Eight

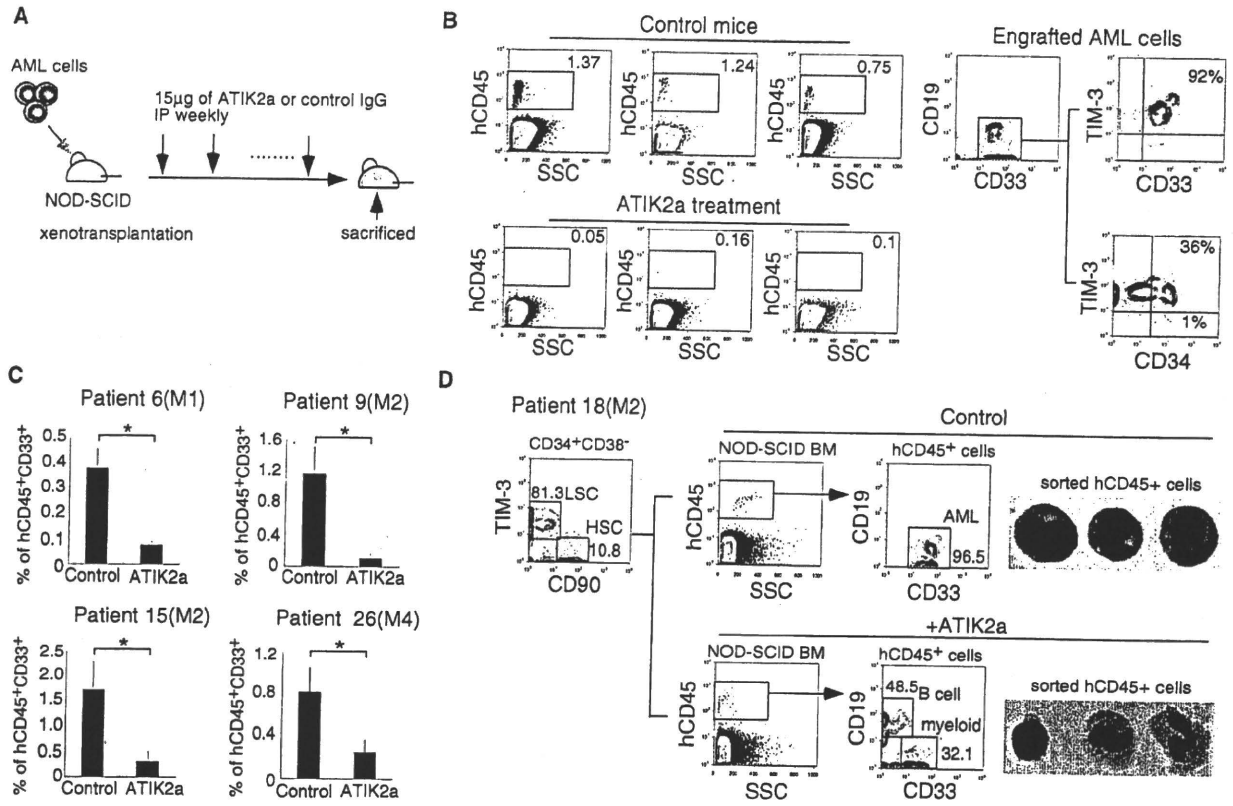

Figure 6. ATIK2a Antibodies Blocked AML Reconstitution in NOD-SCID Mice

(A) Schedule of ATIK2a administration in NOD-SCID experiment. ATIK2a treatment was started 12 hr after the transplantation.

(B) Analysis of mice transplanted with AML bone marrow cells at 16 weeks after transplantation. Three control mice (left top) showed reconstitution of human $CD45^+$ cells, and the majority of these cells were $TIM\text{-}3^+CD33^+$ AML cells that contained $CD34^+$ leukemic progenitor or stem cell populations (right). In contrast, mice treated with ATIK2a (left bottom) have only a small number of $hCD45^+$ cells. Representative data of patient 9 are shown.

(C) Summary of four independent experiments to test the effect of ATIK2a on reconstitution of AML bone marrow cells from patients 6, 9, 15, and 26. In all experiments, ATIK2a treatment significantly inhibited the AML reconstitution. Three mice per group were analyzed.

(D) Selective inhibition of AML reconstitution by ATIK2a in mice reconstituted with the bone marrow of patient 18, which contained both normal HSCs and AML LSCs (left). Injection of the bone marrow cells resulted in AML development in control mice (right top), whereas mice treated with ATIK2a developed normal hematopoiesis (right bottom).

weeks after injection of 10^6 AML cells, engraftment of human AML cells were confirmed by blood sampling. In NRG mice, ATIK2a cannot fully exert its ADCC effects because of a lack of NK cells. Therefore, we injected a high dose (80 μg) of ATIK2a to maximize its CDC effects on AML cells in vivo. These mice were treated with ATIK2a or control IgG, 3 times a week for 4 weeks (Figure 7A). In all four cases tested (patients 7, 14, 27, and 28), ATIK2a treatment significantly reduced human $CD45^+$ AML burden in vivo: ATIK2a strongly suppressed or eliminated the $TIM\text{-}3^+$ AML fraction (Figure 7B, left) that contains all functional LSCs in our hand (Figure 3B), as well as the $CD34^+CD38^-$ LSC fraction (Figure 7B, right, and Figure 7C), suggesting that reduction of leukemic burden by ATIK2a was achieved at least in part by killing LSCs.

In patients 7 and 27, in order to verify the anti-AML LSC effect of ATIK2a treatment, 10^6 human $CD45^+$ AML cells from the primary NRG recipients were further retransplanted into secondary NRG recipients. In patients 14 and 28, however, reduction of AML cells by ATIK2a in primary recipients was very severe, and we could not harvest sufficient numbers of AML cells to transplant into secondary recipients. We then evaluated the re-engraftment of AML cells in secondary recipients 8 weeks after transplantation. All seven mice transplanted with bone marrow cells from primary recipients treated with control IgG developed AML, whereas none of 10 mice transplanted with cells from ATIK2a-treated primary recipients developed AML. Representative data in patient 27 are shown in Figure 7C. These data again suggest that functional LSCs were effectively eliminated by ATIK2a treatment in primary recipients.

DISCUSSION

To selectively kill AML LSCs sparing normal HSCs, one of the most practical approaches is to target the AML LSC-specific surface or functionally indispensable molecules. To achieve specificity for LSCs, the target molecule should be expressed

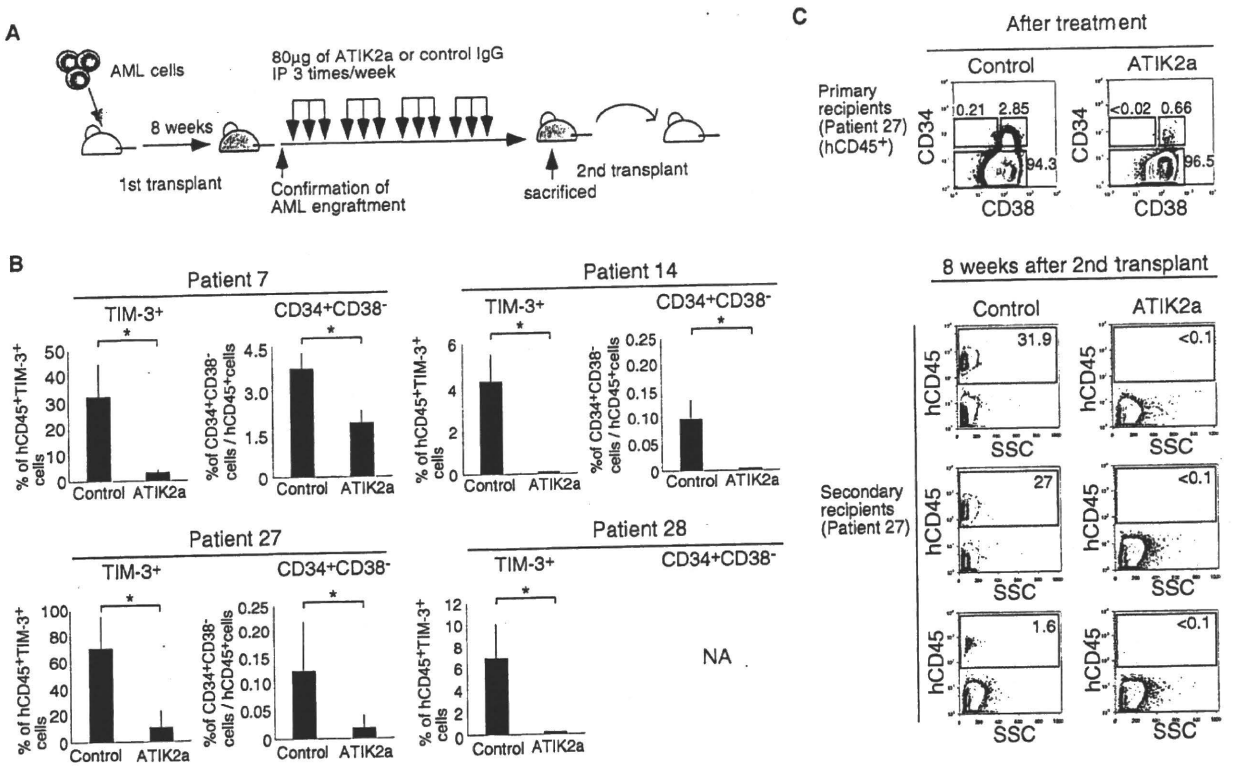

Figure 7. ATIK2a Antibodies Reduced the AML Burden at Least Targeting Functional LSCs

(A) Schedule of ATIK2a administration to test the effect on established human AML in NRG mouse experiments. ATIK2a treatment was started 8 weeks after transplantation.

(B) Summary of four independent experiments to assess the effect of ATIK2a on established human AML cells in vivo (patients 7, 14, 27, and 28). In all experiments, ATIK2a treatment significantly reduced hCD45$^+$ AML burden. Within the hCD45$^+$ population, the TIM-3$^+$ AML fraction that should contain AML LSCs (see Figure 3) was also reduced by this treatment. The percentages of CD34$^+$CD38$^-$ cells, in which LSCs were concentrated, were also reduced. Three to six mice in each group were analyzed.

(C) The phenotype of engrafted hCD45$^+$ cells in primary recipients (top). 10^6 hCD45$^+$ AML cells were then harvested from primary recipients treated with ATIK2a or control IgG, and then retransplanted into the secondary NRG recipients. ATIK2a efficiently blocked reconstitution of AML cells (bottom). Representative results of patient 27 are shown.

on LSCs at a high level but not on normal HSCs. In addition, when the molecule is expressed also in leukemic progenitors or blasts, it will help mass reduction of AML clones. It should not matter whether the molecule is expressed in normal mature blood cells or progenitor cells, because if normal HSCs are spared, they should be able to replenish all mature blood cells after treatment.

TIM-3 is expressed in the CD34$^+$CD38$^-$ AML LSC fraction as well as the majority of their downstream CD38$^+$ leukemic progenitors in most AML types except for M3. TIM-3$^+$ but not TIM-3$^-$ AML population engrafted and reconstituted human AML in NRG mice, suggesting that functional LSCs almost exclusively reside in TIM-3$^+$ cells. In contrast, normal HSCs do not express TIM-3. Thus, TIM-3 should be useful molecules to target AML LSCs without seriously affecting normal hematopoiesis. In steady-state human hematopoiesis, TIM-3 is not expressed in HSCs or myeloerythroid or lymphoid progenitor populations. TIM-3 expression begins at the GMP stage, in parallel with monocyte lineage commitment (Figure 4). Furthermore, in addition to TIM-3, the expression profiling data show that the CD34$^+$ CD38$^-$ LSC fraction expressed many monocyte lineage-related molecules such as CD86 and CSF1R at a high level (Figure 1). In this context, LSCs in most AML types, except for M3 that might be of granulocytic lineage leukemia, may activate some monocyte lineage-related programs.

ATIK2a, a TIM-3 antibody with ADCC and CDC activities, selectively blocked the human AML engraftment and/or development in NOD-SCID mice, whereas it did not disturb normal HSC engraftment. Furthermore, in NRG mice transplanted with human AML cells where percentage of engrafted human cells reached 5%–60% (Figure 7B), ATIK2a treatment reduced or eliminated CD34$^+$ CD38$^-$ and TIM-3$^+$ LSC-containing fractions within the bone marrow of primary recipients, resulting in failure of re-engraftment of primary recipients' bone marrow cells into secondary recipients (Figure 7C). Collectively, it is likely that ATIK2a eradicated functional AML LSCs in vivo, sparing normal HSCs.

To use surface markers for targeting AML LSCs, specificity as well as sensitivity should be critical. TIM-3 has an advantage against other candidate markers in several aspects: Detectable levels of TIM-3 protein is not expressed in normal HSCs or other

progenitors except for only a fraction of GMPs. Furthermore, TIM-3 is expressed in LSCs at a high level, and its expression was found in the vast majority of $CD34^+CD38^-$ cells of M0, M1, M2, and M4 AMLs in all cases tested. As shown in Figure 1, the mRNA expression level of CD25, CD32, CD44, and CD47 in LSCs was only 2- to 3-fold higher as compared to normal HSCs, and in some AML cases, LSCs did not express these molecules. CD33 and CD123 proteins were detectable in normal HSCs (Figure 1B) as well as most myeloid progenitors including CMPs and GMPs (Taussig et al., 2005). In fact, prolonged cytopenias have been observed in AML patients treated with gemtuzumab, a recombinant humanized CD33 monoclonal antibody conjugated with the cytotoxic antibiotic calicheamicin, and this side effect could be due to CD33 expression in normal HSCs (Taussig et al., 2005). CLL-1, CSF1R, TIM-3, and CD96 are the group of molecules that are specifically expressed in LSCs. Among all, the sensitivity of TIM-3 is likely to be the highest at least for AML M0, M1, M2, and M4 (Figures 1B and 2). Thus, TIM-3 might be one of the most useful therapeutic targets at least for these AML types.

It may also be important to understand function of these molecules in maintenance or reconstitution capability of LSCs. For example, it was shown that CD44 monoclonal antibodies reduced the leukemic burden and blocked secondary engraftment in a NOD-SCID model (Jin et al., 2006). This effect on LSCs was mediated in part by the disruption of LSC-niche interactions (Jin et al., 2006). CD47 antibodies can block LSC reconstitution and inhibited the growth of engrafted human AML in a NOD-SCID model (Majeti et al., 2009). However, the interpretation of this result is difficult because the anti-LSC effect of CD47 antibody treatment in this xenograft model could be due to induction of xenogeneic rejection by blocking the ligation of human CD47 expressed on LSCs with mouse SIRPA: NOD-type SIRPA expressed on host macrophage is agonistic for human CD47 to block phagocytotic signals, resulting in the induction of tolerance for human cells in this model (Takenaka et al., 2007). The effect of TIM-3 antibodies in our study might be due to killing activity for their target cells that should include LSCs. It is, however, still important to understand the role of TIM-3 signaling in LSC functions by, for example, testing the effect of activation or suppression of TIM-3 signaling on LSC fate decision.

In summary, TIM-3 is a promising surface molecule to target AML LSCs of most FAB types. Our in vivo experiments strongly suggest that targeting this molecule by monoclonal antibody treatment is a practical approach to eradicate human AML.

EXPERIMENTAL PROCEDURES

Clinical Samples

The bone marrow samples of 34 adult AML cases diagnosed according to French-American-British (FAB) and WHO criteria were enrolled. Human adult bone marrow and peripheral blood cells were obtained from healthy donors. Cord blood cells were obtained from full-term deliveries. Informed consent was obtained from all patients and controls in accordance with the Helsinki Declaration of 1975 that was revised in 1983. The Institutional Review Board of Kyushu University Hospital approved all research on human subjects.

Antibodies, Cell Staining, and Sorting

For the analyses and sorting of human HSCs and progenitors, cells were stained and sorted by FACS Aria (BD Biosciences) as we have previously reported (Kikushige et al., 2008; Yoshimoto et al., 2009). In brief, for the analyses and sorting of HSCs and myeloid progenitors, cells were stained with a Cy5-PE- or PC5-conjugated lineage cocktail, including anti-CD3 (HIT3a), CD4 (RPA-T4), CD8 (RPA-T8), CD10 (HI10a), CD19 (HIB19), CD20 (2H7), CD11b (ICFR44), CD14 (RMO52), CD56 (NKH-1), and GPA (GA-R2); FITC-conjugated anti-CD34 (8G12), anti-CD90 (5E10), or anti-CD45RA (HI100); PE-conjugated anti-TIM-3 (344823), CD33 (HIM3-4), CD96 (NK92.39), or anti-CD123 (6H6); APC-conjugated anti-CD34 (8G12) or anti-CD38 (HIT2); and Pacific Blue conjugated anti-CD45RA (HI100), and biotinylated anti-CD38 (HIT2), or anti-CD123 (9F5). For analysis and sorting of human cells in the immunodeficient mice, FITC-conjugated anti-CD33 (HIM3-4), PE-conjugated anti-CD19 (HIB19), PE-Cy7-conjugated anti-CD38 (HIT2), and APC-conjugated anti-CD45 (J.33) monoclonal antibodies were used in addition to the antibodies described above. Streptavidin-conjugated APC-Cy7 or PE-Cy7 was used for visualization of the biotinylated antibodies (BD PharMingen, San Jose, CA). Nonviable cells were excluded by propidium iodide (PI) staining. Appropriate isotype-matched, irrelevant control monoclonal antibodies were used to determine the level of background staining. The cells were sorted and analyzed by FACS Aria (BD Biosciences, San Jose, CA). The sorted cells were subjected to an additional round of sorting withthe same gate to eliminate contaminating cells and doublets. For single-cell assays, an automatic cell-deposition unit system (BD Biosciences, San Jose, CA) was used.

In Vitro Assays to Determine the Differentiation Potential of Myeloid Progenitors

Clonogenic colony-forming unit (CFU) assays were performed with a methylcellulose culture system that was set up to detect all possible outcomes of myeloid differentiation as reported previously (Kikushige et al., 2008; Manz et al., 2002). Colony numbers were enumerated on day 14 of culture. All of the cultures were incubated at 37°C in a humidified chamber under 5% CO_2.

Microarray Analysis

Twelve AML samples and five normal adult HSCs samples were investigated with Sentrix Bead Chip Assay For Gene Expression, Human-6 V2 (Illumina). In brief, total RNA was extracted with TRIzol (Invitrogen) from FACS-sorted AML $CD34^+CD38^-$ cells and normal $CD34^+CD38^-Lin^-$ HSCs, and biotinylated complementary RNA was synthesized with two round amplification steps via MessageAmpII aRNA Amplification Kit and Illumina TotalPrep RNA Amplification Kit (Applied Biosystems). 1.5 μg of cRNA from each sample was hybridized to the Bead Chip. After staining and washing, Bead Chip was scanned with an Illumina Bead Array reader. Microarray data were analyzed with Gene Spring GX11.01 software (Agilent Technologies). According to the guided workflow for Illumina single color experiment, normalization algorithm of 75-percentile shift was used, and the preprocessing baseline was adjusted to median of all samples.

Production of Recombinant Anti-Human TIM-3 Mouse Monoclonal Antibody

Human TIM-3 cDNA were cloned from normal pancreas cDNA (Clontech). Female Balb/C mouse (7-week-old, Purchased from Charles River) was immunized with L929 cells stably expressing TIM-3 four times and soluble human TIM-3 protein once. Four days after the final injection, spleen cells were fused with SP2/O cells by the PEG method and selected in the HAT-medium. Hybridomas were screened by FACS and clone-sorted. cDNAs encoding the variable regions amplified by SMART RACE cDNA Kit (Clontech) and specific primers (Doenecke et al., 1997) were ligated to mouse IgG2a or Igκ constant region.

Evaluation of ADCC and CDC Activities of ATIK2a Antibodies

ADCC and CDC were determined as previously described with slight modification (Shields et al., 2001; Tawara et al., 2008). For ADCC, target cells and IL-2-cultured peripheral blood mononuclear cells prepared from healthy volunteers were incubated with antibodies (1 μg/mL, Effecter/Target ratio = 25). Cytotoxicity was analyzed by CytoTox 96 Non-Radioactive Cytotoxicity Assay (Promega) as follows: specific lysis [%] = $(A_E - A_{Allo})/(A_{Max} - A_{TS}) \times 100$, where A_E is absorbance of experiment, A_{Allo} is allogenic reaction (no antibody control), A_{Max} is maximum, A_{TS} is target spontaneous release. For CDC, viability of target cells incubated with rabbit sera was assayed by CellTiterGlo (Promega, no antibody control = 100%). UPC 10 (Sigma) replaced in PBS was used as an isotype control.

Transplantation of AML Cells into Immunodeficient Mice

NOD-SCID and NRG mice (stock#7799) were purchased from The Jackson Laboratory. The mice were housed in a specific-pathogen-free facility in micro-isolator cages at the Kyushu University. Animal experiments were performed in accordance with institutional guidelines approved by the Kyushu University animal care committee. NOD-SCID and NRG mice were irradiated at a sublethal dose (2.4 Gy and 4.8 Gy, respectively). In transplantation of AML cells, NOD-SCID mice additionally received a single intraperitoneal injection of 200 μg purified CD122 antibodies that were generated from TM-β1 hybridoma (Tanaka et al., 1993) before transplantation, based on the expectation that it induces transient reduction of NK cells and helps human cell engraftment. We did not inject CD122 antibodies in transplantion of normal bone marrow or cord blood cells. AML cells or $CD34^+$ cells from adult bone marrow and cord blood cells were transplanted via a tail vein.

Statistical Analysis

Data were presented as the mean ± standard deviation. The significance of the differences between groups was determined via Student's t test.

ACCESSION NUMBERS

The microarray data are available in the Gene Expression Omnibus (GEO) database (http://www.ncbi.nlm.nih.gov/gds) under the accession number 24395.

SUPPLEMENTAL INFORMATION

Supplemental Information includes two tables and can be found with this article online at doi:10.1016/j.stem.2010.11.014.

ACKNOWLEDGMENTS

This work was supported in part by a Grant-in-Aid from the Ministry of Education, Culture, Sports, Science and Technology in Japan. S.-i.T. and Y.I. are employees of Kyowa Hakko Kirin Co., Ltd.

Received: February 25, 2010
Revised: August 23, 2010
Accepted: October 6, 2010
Published: December 2, 2010

REFERENCES

Aikawa, Y., Katsumoto, T., Zhang, P., Shima, H., Shino, M., Terui, K., Ito, E., Ohno, H., Stanley, E.R., Singh, H., et al. (2010). PU.1-mediated upregulation of CSF1R is crucial for leukemia stem cell potential induced by MOZ-TIF2. Nat. Med. *16*, 580–585, 1p, 585.

Anderson, A.C., Anderson, D.E., Bregoli, L., Hastings, W.D., Kassam, N., Lei, C., Chandwaskar, R., Karman, J., Su, E.W., Hirashima, M., et al. (2007). Promotion of tissue inflammation by the immune receptor Tim-3 expressed on innate immune cells. Science *318*, 1141–1143.

Bhatia, M., Wang, J.C., Kapp, U., Bonnet, D., and Dick, J.E. (1997). Purification of primitive human hematopoietic cells capable of repopulating immune-deficient mice. Proc. Natl. Acad. Sci. USA *94*, 5320–5325.

Bonnet, D., and Dick, J.E. (1997). Human acute myeloid leukemia is organized as a hierarchy that originates from a primitive hematopoietic cell. Nat. Med. *3*, 730–737.

Doenecke, A., Winnacker, E.L., and Hallek, M. (1997). Rapid amplification of cDNA ends (RACE) improves the PCR-based isolation of immunoglobulin variable region genes from murine and human lymphoma cells and cell lines. Leukemia *11*, 1787–1792.

Florian, S., Sonneck, K., Hauswirth, A.W., Krauth, M.T., Schernthaner, G.H., Sperr, W.R., and Valent, P. (2006). Detection of molecular targets on the surface of CD34+/CD38-/- stem cells in various myeloid malignancies. Leuk. Lymphoma *47*, 207–222.

Hauswirth, A.W., Florian, S., Printz, D., Sotlar, K., Krauth, M.T., Fritsch, G., Schernthaner, G.H., Wacheck, V., Selzer, E., Sperr, W.R., and Valent, P. (2007). Expression of the target receptor CD33 in CD34+/CD38-/CD123+ AML stem cells. Eur. J. Clin. Invest. *37*, 73–82.

Hope, K.J., Jin, L., and Dick, J.E. (2004). Acute myeloid leukemia originates from a hierarchy of leukemic stem cell classes that differ in self-renewal capacity. Nat. Immunol. *5*, 738–743.

Hosen, N., Park, C.Y., Tatsumi, N., Oji, Y., Sugiyama, H., Gramatzki, M., Krensky, A.M., and Weissman, I.L. (2007). CD96 is a leukemic stem cell-specific marker in human acute myeloid leukemia. Proc. Natl. Acad. Sci. USA *104*, 11008–11013.

Ishikawa, F., Yasukawa, M., Lyons, B., Yoshida, S., Miyamoto, T., Yoshimoto, G., Watanabe, T., Akashi, K., Shultz, L.D., and Harada, M. (2005). Development of functional human blood and immune systems in NOD/SCID/IL2 receptor gamma chain(null) mice. Blood *106*, 1565–1573.

Ishikawa, F., Yoshida, S., Saito, Y., Hijikata, A., Kitamura, H., Tanaka, S., Nakamura, R., Tanaka, T., Tomiyama, H., Saito, N., et al. (2007). Chemotherapy-resistant human AML stem cells home to and engraft within the bone-marrow endosteal region. Nat. Biotechnol. *25*, 1315–1321.

Jaiswal, S., Jamieson, C.H., Pang, W.W., Park, C.Y., Chao, M.P., Majeti, R., Traver, D., van Rooijen, N., and Weissman, I.L. (2009). CD47 is upregulated on circulating hematopoietic stem cells and leukemia cells to avoid phagocytosis. Cell *138*, 271–285.

Jin, L., Hope, K.J., Zhai, Q., Smadja-Joffe, F., and Dick, J.E. (2006). Targeting of CD44 eradicates human acute myeloid leukemic stem cells. Nat. Med. *12*, 1167–1174.

Jin, L., Lee, E.M., Ramshaw, H.S., Busfield, S.J., Peoppl, A.G., Wilkinson, L., Guthridge, M.A., Thomas, D., Barry, E.F., Boyd, A., et al. (2009). Monoclonal antibody-mediated targeting of CD123, IL-3 receptor alpha chain, eliminates human acute myeloid leukemic stem cells. Cell Stem Cell *5*, 31–42.

Kikushige, Y., Yoshimoto, G., Miyamoto, T., Iino, T., Mori, Y., Iwasaki, H., Niiro, H., Takenaka, K., Nagafuji, K., Harada, M., et al. (2008). Human Flt3 is expressed at the hematopoietic stem cell and the granulocyte/macrophage progenitor stages to maintain cell survival. J. Immunol. *180*, 7358–7367.

Krause, D.S., and Van Etten, R.A. (2007). Right on target: Eradicating leukemic stem cells. Trends Mol. Med. *13*, 470–481.

Lapidot, T., Sirard, C., Vormoor, J., Murdoch, B., Hoang, T., Caceres-Cortes, J., Minden, M., Paterson, B., Caligiuri, M.A., and Dick, J.E. (1994). A cell initiating human acute myeloid leukaemia after transplantation into SCID mice. Nature *367*, 645–648.

Majeti, R., Chao, M.P., Alizadeh, A.A., Pang, W.W., Jaiswal, S., Gibbs, K.D., Jr., van Rooijen, N., and Weissman, I.L. (2009). CD47 is an adverse prognostic factor and therapeutic antibody target on human acute myeloid leukemia stem cells. Cell *138*, 286–299.

Manz, M.G., Miyamoto, T., Akashi, K., and Weissman, I.L. (2002). Prospective isolation of human clonogenic common myeloid progenitors. Proc. Natl. Acad. Sci. USA *99*, 11872–11877.

Martelli, M.P., Pettirossi, V., Thiede, C., Bonifacio, E., Mezzasoma, F., Cecchini, D., Pacini, R., Tabarrini, A., Ciurnelli, R., Gionfriddo, I., et al. (2010). CD34+ cells from AML with mutated NPM1 harbor cytoplasmic mutated nucleophosmin and generate leukemia in immunocompromised mice. Blood Press. Published online July 15, 2010. 10.1182/blood-2009-08-238899.

Monney, L., Sabatos, C.A., Gaglia, J.L., Ryu, A., Waldner, H., Chernova, T., Manning, S., Greenfield, E.A., Coyle, A.J., Sobel, R.A., et al. (2002). Th1-specific cell surface protein Tim-3 regulates macrophage activation and severity of an autoimmune disease. Nature *415*, 536–541.

Nakae, S., Iikura, M., Suto, H., Akiba, H., Umetsu, D.T., Dekruyff, R.H., Saito, H., and Galli, S.J. (2007). TIM-1 and TIM-3 enhancement of Th2 cytokine production by mast cells. Blood *110*, 2565–2568.

Nakayama, M., Akiba, H., Takeda, K., Kojima, Y., Hashiguchi, M., Azuma, M., Yagita, H., and Okumura, K. (2009). Tim-3 mediates phagocytosis of apoptotic cells and cross-presentation. Blood *113*, 3821–3830.

Nimmerjahn, F., and Ravetch, J.V. (2005). Divergent immunoglobulin g subclass activity through selective Fc receptor binding. Science *310*, 1510–1512.

Nimmerjahn, F., and Ravetch, J.V. (2007). Antibodies, Fc receptors and cancer. Curr. Opin. Immunol. *19*, 239–245.

Pearson, T., Shultz, L.D., Miller, D., King, M., Laning, J., Fodor, W., Cuthbert, A., Burzenski, L., Gott, B., Lyons, B., et al. (2008). Non-obese diabetic-recombination activating gene-1 (NOD-Rag1 null) interleukin (IL)-2 receptor common gamma chain (IL2r gamma null) null mice: A radioresistant model for human lymphohaematopoietic engraftment. Clin. Exp. Immunol. *154*, 270–284.

Sabatos, C.A., Chakravarti, S., Cha, E., Schubart, A., Sánchez-Fueyo, A., Zheng, X.X., Coyle, A.J., Strom, T.B., Freeman, G.J., and Kuchroo, V.K. (2003). Interaction of Tim-3 and Tim-3 ligand regulates T helper type 1 responses and induction of peripheral tolerance. Nat. Immunol. *4*, 1102–1110.

Saito, Y., Kitamura, H., Hijikata, A., Tomizawa-Murasawa, M., Tanaka, S., Takagi, S., Uchida, N., Suzuki, N., Sone, A., Najima, Y., et al. (2010). Identification of therapeutic targets for quiescent, chemotherapy-resistant human leukemia stem cells. Sci. Transl. Med. *2*, ra9.

Sánchez-Fueyo, A., Tian, J., Picarella, D., Domenig, C., Zheng, X.X., Sabatos, C.A., Manlongat, N., Bender, O., Kamradt, T., Kuchroo, V.K., et al. (2003). Tim-3 inhibits T helper type 1-mediated auto- and alloimmune responses and promotes immunological tolerance. Nat. Immunol. *4*, 1093–1101.

Shields, R.L., Namenuk, A.K., Hong, K., Meng, Y.G., Rae, J., Briggs, J., Xie, D., Lai, J., Stadlen, A., Li, B., et al. (2001). High resolution mapping of the binding site on human IgG1 for Fc gamma RI, Fc gamma RII, Fc gamma RIII, and FcRn and design of IgG1 variants with improved binding to the Fc gamma R. J. Biol. Chem. *276*, 6591–6604.

Takenaka, K., Prasolava, T.K., Wang, J.C., Mortin-Toth, S.M., Khalouei, S., Gan, O.I., Dick, J.E., and Danska, J.S. (2007). Polymorphism in Sirpa modulates engraftment of human hematopoietic stem cells. Nat. Immunol. *8*, 1313–1323.

Tanaka, T., Kitamura, F., Nagasaka, Y., Kuida, K., Suwa, H., and Miyasaka, M. (1993). Selective long-term elimination of natural killer cells in vivo by an anti-interleukin 2 receptor beta chain monoclonal antibody in mice. J. Exp. Med. *178*, 1103–1107.

Taussig, D.C., Pearce, D.J., Simpson, C., Rohatiner, A.Z., Lister, T.A., Kelly, G., Luongo, J.L., Danet-Desnoyers, G.A., and Bonnet, D. (2005). Hematopoietic stem cells express multiple myeloid markers: Implications for the origin and targeted therapy of acute myeloid leukemia. Blood *106*, 4086–4092.

Taussig, D.C., Miraki-Moud, F., Anjos-Afonso, F., Pearce, D.J., Allen, K., Ridler, C., Lillington, D., Oakervee, H., Cavenagh, J., Agrawal, S.G., et al. (2008). Anti-CD38 antibody-mediated clearance of human repopulating cells masks the heterogeneity of leukemia-initiating cells. Blood *112*, 568–575.

Taussig, D.C., Vargaftig, J., Miraki-Moud, F., Griessinger, E., Sharrock, K., Luke, T., Lillington, D., Oakervee, H., Cavenagh, J., Agrawal, S.G., et al. (2010). Leukemia-initiating cells from some acute myeloid leukemia patients with mutated nucleophosmin reside in the CD34(-) fraction. Blood *115*, 1976–1984.

Tawara, T., Hasegawa, K., Sugiura, Y., Harada, K., Miura, T., Hayashi, S., Tahara, T., Ishikawa, M., Yoshida, H., Kubo, K., et al. (2008). Complement activation plays a key role in antibody-induced infusion toxicity in monkeys and rats. J. Immunol. *180*, 2294–2298.

Uchida, J., Hamaguchi, Y., Oliver, J.A., Ravetch, J.V., Poe, J.C., Haas, K.M., and Tedder, T.F. (2004). The innate mononuclear phagocyte network depletes B lymphocytes through Fc receptor-dependent mechanisms during anti-CD20 antibody immunotherapy. J. Exp. Med. *199*, 1659–1669.

van Rhenen, A., van Dongen, G.A., Kelder, A., Rombouts, E.J., Feller, N., Moshaver, B., Stigter-van Walsum, M., Zweegman, S., Ossenkoppele, G.J., and Jan Schuurhuis, G. (2007). The novel AML stem cell associated antigen CLL-1 aids in discrimination between normal and leukemic stem cells. Blood *110*, 2659–2666.

Yalcintepe, L., Frankel, A.E., and Hogge, D.E. (2006). Expression of interleukin-3 receptor subunits on defined subpopulations of acute myeloid leukemia blasts predicts the cytotoxicity of diphtheria toxin interleukin-3 fusion protein against malignant progenitors that engraft in immunodeficient mice. Blood *108*, 3530–3537.

Yoshimoto, G., Miyamoto, T., Jabbarzadeh-Tabrizi, S., Iino, T., Rocnik, J.L., Kikushige, Y., Mori, Y., Shima, T., Iwasaki, H., Takenaka, K., et al. (2009). FLT3-ITD up-regulates MCL-1 to promote survival of stem cells in acute myeloid leukemia via FLT3-ITD-specific STAT5 activation. Blood *114*, 5034–5043.

Cancer Science
The official journal of the Japanese Cancer Association JCA

Suppression of gastric cancer dissemination by ephrin-B1-derived peptide

Masamitsu Tanaka,[1,3] Reiko Kamata,[1] Kazuyoshi Yanagihara[2] and Ryuichi Sakai[1,4]

[1]Department of Growth Factor Division, [2]Central Animal Laboratory, National Cancer Center Research Institute, Tokyo; [3]Department of Molecular Medicine and Biochemistry, Akita University Graduate School of Medicine, Akita, Japan

(Received May 1, 2009/Revised August 27, 2009/Accepted September 1, 2009/Online publication October 4, 2009)

Interaction of the Eph family of receptor protein tyrosine kinases and their ligands, ephrin family members, induces bidirectional signaling through cell–cell contacts. High expression of B-type ephrin is associated with high invasion potential of tumors, and we previously observed that signaling through the C-terminus of ephrin-B1 mediates the migration and invasion of cells, and is involved in the promotion of carcinomatous peritonitis *in vivo*. Here we show that the intracellular introduction of a synthetic peptide derived from ephrin-B1 C-terminus blocks ephrin-B1 mediated signaling in scirrhous gastric cancer cells. Treatment of cancer cells with a fusion peptide consisting of HIV-TAT and amino acids 331–346 of ephrin-B1 (PTD-EFNB1-C) suppressed the activation of RhoA, mediated by the association of ephrin-B1 with an adaptor protein Dishevelled, and also inhibited extracellular secretion of metalloproteinase. Moreover, injection of PTD-EFNB1-C peptide into the peritoneal cavity of nude mice suppressed carcinomatous peritonitis of intraperitoneally transplanted scirrhous gastric cancer cells. These results indicate the possible application of ephrin-B1 C-terminal peptide to develop novel protein therapy for scirrhous gastric carcinoma, especially in the stage of tumor progression, including peritoneal dissemination. (*Cancer Sci* 2010; 101: 87–93)

The members of the Eph receptor family can be classified into two groups based on their sequence similarity and their preferential binding to ligands tethered to the cell surface either by a glycosylphosphatidyl inositol-anchor (ephrin-A) or a transmembrane domain (ephrin-B).[1–3] The interaction of EphB receptor protein tyrosine kinases and their ephrin-B ligands induces bidirectional signaling through the resultant cell–cell contacts. Ephrin-B has an intracellular domain that includes sites for tyrosine phosphorylation by means of Src family kinases and a docking site for proteins with a PDZ domain.[4–6] These sites give ephrin-B ligands at least two ways of involving intracellular signaling. In addition, we and others previously reported that the association of Dishevelled with the C-terminal region of ephrin-B1, which was independent of the PDZ domain, affects the cell motility through regulation of the small GTPase, RhoA.[7–9] Although investigation of the functions of Eph receptors and ephrins have focused on the development of the vascular and nervous systems, the roles of Eph–ephrin pathways in epithelial cells and cancers have also attracted interest.[10–14] Overexpression of B-type ephrin in cancer cells is reported to correlate with high invasion and high vascularity of tumors,[15,16] and elevated expression of ephrin-B1 is observed in poorly differentiated invasive tumor cells and other tumors with poor clinical prognosis.[17,18] As one of the mechanisms of ephrin-B1 mediated enhancement of cancer cell invasion, we previously reported that the C-terminus of ephrin-B1 regulates the exocytosis of MMP-8 in response to the interaction with the EphB2 receptor, which depends on the intracellular signaling including activation of Arf1 GTPase.[19] Because MMP-8 is expressed in wide variety of cells and it cleaves all three α-chains of types I, II, and III collagen as well as a wide range of non-collagenous substrates, regulation of this MMP family member through the ephrin-B1 C-terminus might contribute to the highly invasive phenotype of ephrin-B1 expressing cancer cells by degradation of the extracellular matrix.[20–22]

In order to facilitate the application of ephrin-B1 to develop a novel molecular therapy, the synthetic peptide derived from ephrin-B1 C-terminus was evaluated for its effects on tumor suppression. A 13 amino acid (aa) peptide (GRKKRRQRRRPPQ) derived from the protein transduction domain (PTD) of HIV-TAT elicits transport of its fusion protein through cellular membranes and is generally used for the intracellular delivery of proteins.[23] In this report, we show that a fusion protein consisting of PTD and ephrin-B1$^{331–346}$ attenuates the signaling through ephrin-B1, and suppresses cancer promotion including carcinomatous peritonitis of scirrhous gastric cancer *in vivo*.

Materials and Methods

Plasmids, antibodies and reagents. Plasmids encoding ephrin-B1 and GST-GGA3 have been described previously.[19] Rabbit polyclonal antibody that recognizes ephrin-B1 (C18) was purchased from Santa Cruz Biotechnology (Santa Cruz, CA, USA). The goat polyclonal antibody against ephrin-B1, which reacts with the entire extracellular domain, was purchased from R&D Systems (Minneapolis, MN, USA). Polyclonal antibodies for Dishevelled and HA-epitope were purchased from Santa Cruz Biotechnology. Antibody for MMP-8 was from Millipore (Billerica, MA, USA). Monoclonal antibodies for HIV-TAT$^{47–58}$ and myc-epitope (9E10) were purchased from Abcam (Cambridge, UK) and Santa Cruz, respectively. PTD-EFNB1-C peptide was synthesized as a fusion peptide of HIV-TAT PTD with ephrin-B1 (aa 331–346) connected by a linker GGG; GRKKRRQRRRPPQGGGVQEMPPQSPANIYYKV. As a control, the scrambled sequenced peptide that contains the same aa composition of the PTD-EFNB1-C was synthesized as follows: GRKKRRQRRRPPQGGGEISKPMYPQVQVYPNA.

Cell culture, transfection, and peptide treatment. The 44As3 cell line was cultured in RPMI-1640 supplemented with 10% FBS.[24] Cos1 cells were cultured in DMEM with 10% FBS. For transient expression assays, Cos1 cells were transfected with plasmid DNA using FuGene6 reagent (Invitrogen, Carlsbad, CA, USA). Peptides were added to the cultured cells at the final concentration of 1 or 5 μM.

Cell migration assay and collagen gel invasion assay. Migration assay and collagen gel invasion assay were carried out using Transwell chambers as described previously.[19] The assays were done three times.

RhoA-GTP and Arf1-GTP pull-down assay. The activation of RhoA and Arf1 was examined by affinity precipitation of GTP-bound RhoA with the GST fusion protein of the RhoA binding

[4]To whom correspondence should be addressed. E-mail: rsakai@ncc.go.jp

doi: 10.1111/j.1349-7006.2009.01352.x

domain of Rho kinase (GST-RB), and GTP-Arf1 with GST-tagged GGA3 (GST-GGA3) as described.[7,19]

***In vivo* peritoneal dissemination assay.** The animal experimental protocols were approved by the National Cancer Center Committee for Ethics of Animal Experimentation, and the experiments were conducted in accordance with the guidelines for Animal Experiments in the National Cancer Center (Tokyo, Japan). Peritoneal dissemination of tumors was tested by i.p. injection of 2×10^6 44As3 cells suspended in 0.3 mL RPMI-1640 medium into 6-week-old BALB/c nude mice ($n = 20$; CLEA Japan, Tokyo, Japan). The mice were killed 12 days after injection and peritoneal dissemination was evaluated. When the tumors were treated with the peptides, 6.25 μM PTD-EFNB1-C peptide in 0.4 mL of PBS per body was injected i.p. 3 days post transplantation of cancer cells, and chased every 24 h at the same concentration until the mice were killed.

Immunohistochemical analysis. Tumor tissues disseminated in the peritoneal cavity of nude mice were fixed, and embedded in paraffin. Paraffin blocks were sectioned in slices and subjected to immunohistochemical staining using the indirect polymer method with Envision reagent (Dako, Carpinteria, CA, USA). Antigen retrieval was carried out by placing sections in the citrate buffer and autoclaved according to the manufacturer's instructions. Sections were incubated with specific antibody against PTD of HIV-TAT.

Results

Peptide derived from ephrin-B1 C-terminus attenuates interaction of ephrin-B1 with Dishevelled and activation of RhoA. Our previous observation that ephrin-B1 is involved in promoting the invasion of cancer cells through the signaling including its C-terminal region led us to determine whether the peptide derived from ephrin-B1 C-terminus would affect the invasion of cancer cells.[19] To this end, a fragment of ephrin-B1 C-terminus containing aa 331 to 346 was fused to the PTD peptide derived from HIV-TAT for intracellular delivery through cellular membranes (PTD-EFNB1-C; Fig. 1, top).[23] 44As3, an ephrin-B1 expressing cell line of scirrhous gastric carcinoma, was previously used to evaluate the involvement of ephrin-B1 in carcinomatous peritonitis.[24] When the 44As3 gastric scirrhous carcinoma cells were incubated with the PTD-EFNB1-C fusion peptide or control peptide Scrm, the peptides were diffusely detected in the cytoplasm and also in the nucleus of almost all of the cells within 30 min and thereafter until at least 48 h by immunostaining with anti-HIV-TAT antibody (Fig. 1A,C,E). The partial nuclear localization of the fusion peptide was previously reported as a characteristic feature of PTD of HIV--TAT.[23] The amount of the exogenous C-terminal fragment of ephrin-B1 derived from the peptide was significantly higher than the endogenous wild-type ephrin-B1, which was preferentially localized to the cell membrane, as judged from the comparison of the intensity of the immunostaining with the antibody reactions to the ephrin-B1 C-terminus (Fig. 1B,D,F).

In order to monitor the effect of the PTD-EFNB1-C fusion peptide on ephrin-B1 mediated signaling, the interaction of ephrin-B1 with the adaptor protein Dishevelled, which physically associates with the C-terminus of ephrin-B1, was examined.[7,8] The binding of exogenously expressed ephrin-B1 with Xenopus Dishevelled was inhibited by the addition of the PTD-EFNB1-C peptide onto the transfected cells in a dose-dependent manner, but not by the control peptide Scrm (Fig. 2A, left). The fusion peptide also effectively suppressed the association of endogenous proteins of ephrin-B1 and Dishevelled in 44As3 cells (Fig. 2A, right).

The interaction of ephrin-B1 with Dishevelled causes the activation of small GTPase RhoA.[7,8] Therefore, the biochemical effect of the PTD-EFNB1-C fusion peptide was next evaluated by monitoring the RhoA activation. The amount of activated GTP-bound RhoA was increased by the expression of ephrin-B1 and Dishevelled in Cos1 cells, as expected (Fig. 2B, left). The incubation of these cells with the PTD-EFNB1-C fusion peptide, but not the control PTD peptide, dose-dependently suppressed the activation of RhoA (Fig. 2B, left). Moreover, inhibition of RhoA activity by PTD-EFNB1-C was also detected in 44As3 cells (Fig. 2B, right). These results indicate that PTD-EFNB1-C peptide is effectively incorporated in cultured cells, and blocks the signaling of ephrin-B1/Dishevelled mediated activation of RhoA.

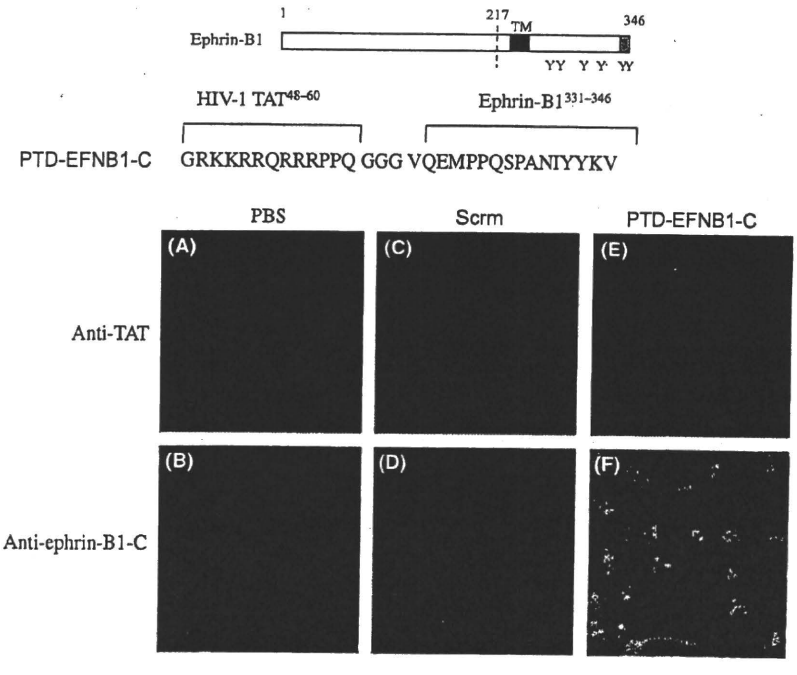

Fig. 1. Top: Diagram of ephrin-B1 and the sequence of a fusion protein consisting of the protein transduction domain of HIV-TAT and ephrin-B1$^{331-346}$ (PTD-EFNB1-C). The gray box at the C-terminus indicates the region required for interaction with Dishevelled. Amino acids 48–60 of HIV-TAT were connected to ephrin-B1$^{331-346}$ using the linker of glycines. TM, transmembrane domain; Y, tyrosine phosphorylation sites. Bottom: Localization of PTD-EFNB1-C peptide in 44As3 scirrhous gastric carcinoma cells. The cells were treated with PTD-EFNB1-C or the control peptide of scrambled sequence (Scrm) for 1 h. The cells were then fixed and subjected to immunostaining with anti-TAT or anti-ephrin-B1 antibody, which reacts to the C-terminus of ephrin-B1, as indicated. Original magnification, ×600.

doi: 10.1111/j.1349-7006.2009.01352.x

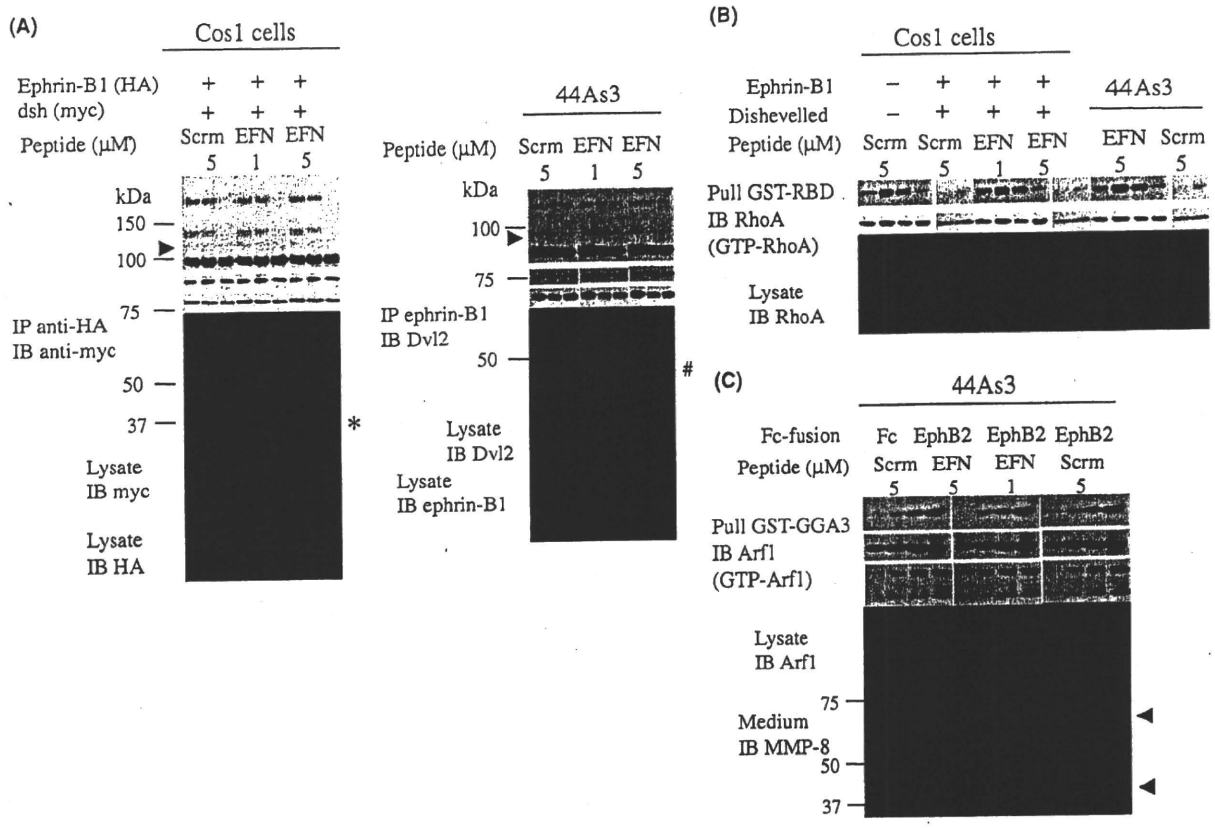

Fig. 2. A fusion protein consisting of the protein transduction domain of HIV-TAT and ephrin-B1$^{331-346}$ (PTD-EFNB1-C) attenuates the association of ephrin-B1 with Dishevelled, and activation of RhoA and Arf1 GTPases. (A) Left: Cos1 cells were transfected with plasmids encoding ephrin-B1 tagged with HA at the C-terminus, and Xenopus Dishevelled (dsh) tagged with six copies of myc-epitope at the N-terminus. The control peptide Scrambled (Scrm) or PTD-EFNB1-C peptide (EFN) was added to the culture medium at the indicated concentrations 10 h after transfection and incubated for 14 h. It should be noted that six copies of the myc-epitope tagged with the cDNA increases the protein size by approximately 8 kDa. Right: 44As3 scirrhous gastric carcinoma cells were treated with the peptides for 24 h. The cells were lysed and subjected to immunoprecipitation (IP) and immunoblotting (IB) with the indicated antibodies. *IgG light chain; #IgG heavy chain. Dvl2, dissevelled 2. (B) Cos1 cells transfected with plasmids and 44As3 cells were treated with peptides as in (A). Cell lysates were subjected to pull-down assay to detect RhoA-GTP with GST-RBD bound to glutathione–Sepharose. The expression of total RhoA in each lysate is shown in the lower panels. (C) Arf1-GTP was pulled with glutathione–Sepharose-conjugated GST-GGA3 from lysates of 44As3 cells treated with peptides as indicated. Expression of the total Arf1 is shown in the middle panel. Bottom: PTD-EFNB1-C decreased MMP-8 secretion. 44As3 cells were treated with the peptide as above, and the conditioned medium was subjected to trichloroacetic acid (TCA) precipitation to detect MMP-8 through immunoblotting. Black arrowhead, proenzyme; white arrowhead, substantially activated MMP-8.

HIV-TAT-ephrinB1 peptide attenuates the secretion of MMP-8 by suppression of Arf1 activity. Signaling mediated by the ephrin-B1 C-terminus affects the secretion of metalloproteinase MMP-8 through activation of Arf1 GTPase in response to the interaction with EphB2, which may lead to degradation of the collagen matrix and assist the invasion of cancer cells.[19] Extracellular secretion of metalloproteinase largely depends on the membrane traffic of secretory granules containing MMPs, and Arf1 is the key molecule to regulate this process.[22] Therefore, we next examined whether the addition of PTD-EFNB1-C modifies Arf1 activation and the secretion of MMP-8. Stimulation of ephrin-B1 is induced by the incubation of ephrin-B1 expressing cells with EphB2-Fc fusion protein, which consists of the extracellular domain of EphB2 with the Fc fragment of mouse IgG2b.[25] The amount of activated GTP-bound Arf1 was increased in ephrin-B1 expressing cells by the treatment of cells with EphB2-Fc, which was inhibited by pretreatment of the cells with PTD-EFNB1-C peptide in 44As3 cells (Fig. 2C). Consistent with this result, the amount of MMP-8 in the culture medium increased by the stimulation with EphB2-Fc, which was also abolished by the preincubation of the cells with PTD-EFNB1-C (Fig. 2C, bottom). However, the amount of MMP-8 mRNA was not altered by the treatment with peptides (data not shown). These results indicate that PTD-EFNB1-C peptide effectively blocked the ephrin-B1 mediated signaling of Arf1 activation, and attenuated the secretion of MMP-8.

PTD-EFNB1-C peptide inhibits invasion of cancer cells *in vitro*. The biological effects of PTD-EFNB1-C peptide were next examined in cultured 44As3 gastric scirrhous carcinoma cells. The incubation of 44As3 cells with the PTD-EFNB1-C peptide suppressed the migration of the cells in a Transwell assay in a dose-dependent manner, whereas the control peptide had no effect (Fig. 3, left). In addition, invasion of 44As3 cells through type I collagen matrix was also significantly abolished by treatment with PTD-EFNB1-C peptide (Fig. 3, right). However, PTD-EFNB1-C did not significantly affect the growth of 44As3 cells under normal cell culture conditions, or the basal apoptosis level of 44As3 cells without additional treatment, which was examined by measurement of nucleosomes in the cytoplasm of apoptotic cells (data not shown). These results suggest that signaling mediated by the C-terminus of ephrin-B1 is involved in cell migration and invasion, rather than the

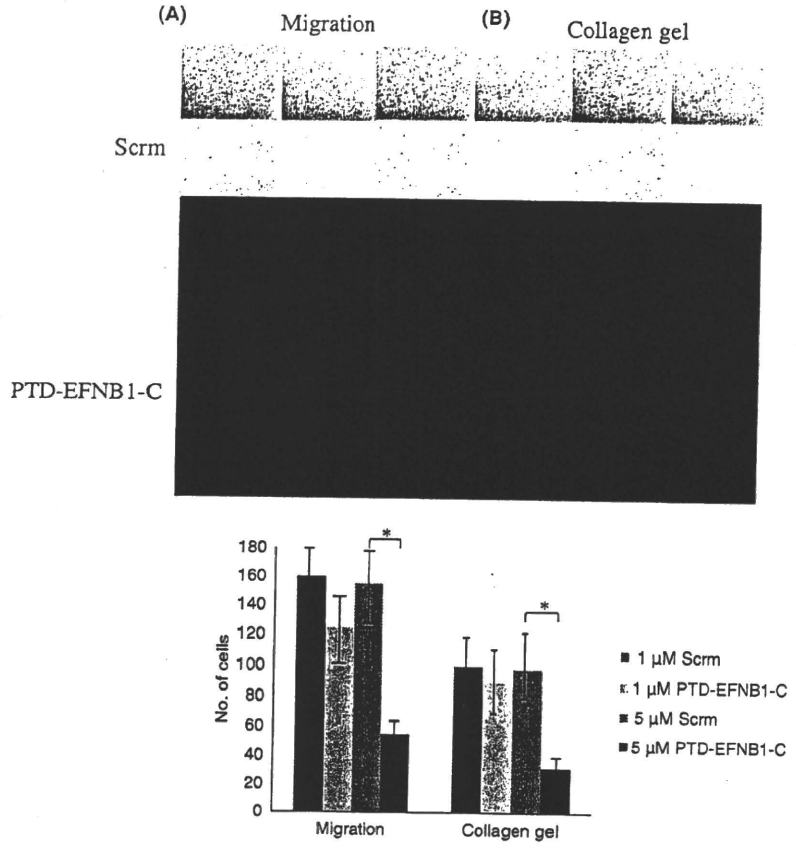

Fig. 3. Fusion protein PTD-EFNB1-C, consisting of the protein transduction domain of HIV-TAT and ephrin-B1$^{331-346}$, attenuates the migration and invasion of 44As3 scirrhous gastric carcinoma cells. 44As3 cells were seeded onto a Transwell membrane in serum-free medium containing control peptide Scrambled (Scrm) or PTD-EFNB1-C at the indicated concentrations. In (B), the Transwell membranes were coated with collagen matrix (25 μg/cm^2). After 10 h (A) or 14 h (B) incubation, the wells were harvested and cells that had moved to the bottom surface of the membrane were counted. Representative fields of experiments with 5 μM of each peptide are shown. The results from three independent experiments, each in duplicate, are shown as the mean ± SD. *$P < 0.01$.

proliferation of cancer cells. This is consistent with our earlier studies that revealed that the expression of ephrin-B1 promotes migration and invasion rather than the proliferation of cancer cells.[19]

PTD-EFNB1-C peptide inhibits the peritoneal dissemination of scirrhous gastric carcinoma. Next, we examined whether PTD-EFNB1-C peptide blocks the cancer promotion *in vivo*. 44As3 cells caused severe peritoneal dissemination after they were transplanted in the peritoneal cavity or orthotopically in the gastric wall of nude mice.[26] Our previous observations that expression of wild-type ephrin-B1, but not the ephrin-B1 mutant, which lacks the four amino acids of its C-terminus, significantly promoted the formation of peritoneal dissemination in nude mice suggested that ephrin-B1 C-terminus mediated signaling stimulates the cancer cell invasion also *in vivo*.[19] Therefore, the effect of PTD-EFNB1-C peptide was examined in the model system of peritoneal dissemination with 44As3 cells.

Following the transplantation of 44As3 cells into the peritoneal cavity of nude mice, PTD-EFNB1-C peptide was injected i.p. 3 days after the transplantation and chased every 24 h until the mice were killed at day 12 (Fig. 4A). Most of the mice transplanted with the 44As3 cells and chased with the control peptide showed significant tumor dissemination in the peritoneal cavity including the mesentery (Fig. 4B), paragastric region (Fig. 4C), and rectouterine region (Fig. 4D), also summarized in Table 1. In contrast, the number and size of disseminated tumor nodules in the mice treated with PTD-EFNB1-C peptide were clearly reduced (Fig. 4B–D, right-hand panels; Tables 1,2). The differences in the number of nodules in mesentery, paragastric, and rectouterine regions were statistically significant ($P < 0.001$) using Pearson's χ^2-test.

When histology of the tumors that developed in the rectouterine region was compared, there was some difference between the groups treated with control peptide and PTD-EFNB1-C. The tumors in control peptide treated mice contained abundant fibrous stromal tissues, which reflects typical human gastric scirrhous carcinoma, whereas the tumors in mice treated with PTD-EFNB1-C contained less volume of stromal fibrosis, and the cancer cells were scattered more diffusely. However, there was no significant change in the level of Ki67, a marker of cell proliferation or apoptosis (as indicated by TUNEL) (Fig. 4D, bottom). The uptake of the control peptide and PTD-EFNB1-C in tumors was further monitored by immunostaining of tumor plaques in the peritoneal cavity with anti HIV-TAT antibody. As shown in Figure 4E, the peptides were detected not only in the outermost surface layer, but also throughout in the tumor plaques. Although the intensity of the staining was variable within the tumor tissues, nearly 40% of the cancer cells were positive for HIV-TAT immunostaining (Fig. 4E).

Discussion

In this study, we showed that the peptide derived from ephrin-B1 C-terminus fused with PTD peptide of HIV-TAT was sufficient to cause apparent inhibition of peritoneal dissemination of 44As3 cells. Because PTD-EFNB1-C is diffusely distributed in the cytoplasm, it is likely the peptide captured the downstream effector proteins that interact with the C-terminus of ephrin-B1, and prevented the physical association of these effectors with wild type ephrin-B1. For example, four amino acids of ephrin-B1 C-terminus are necessary for the interaction of ephrin-B1 with Dishevelled,[8] which was effectively blocked by the addition of PTD-EFNB1-C. The fact that PTD-EFNB1-C peptide

doi: 10.1111/j.1349-7006.2009.01352.x

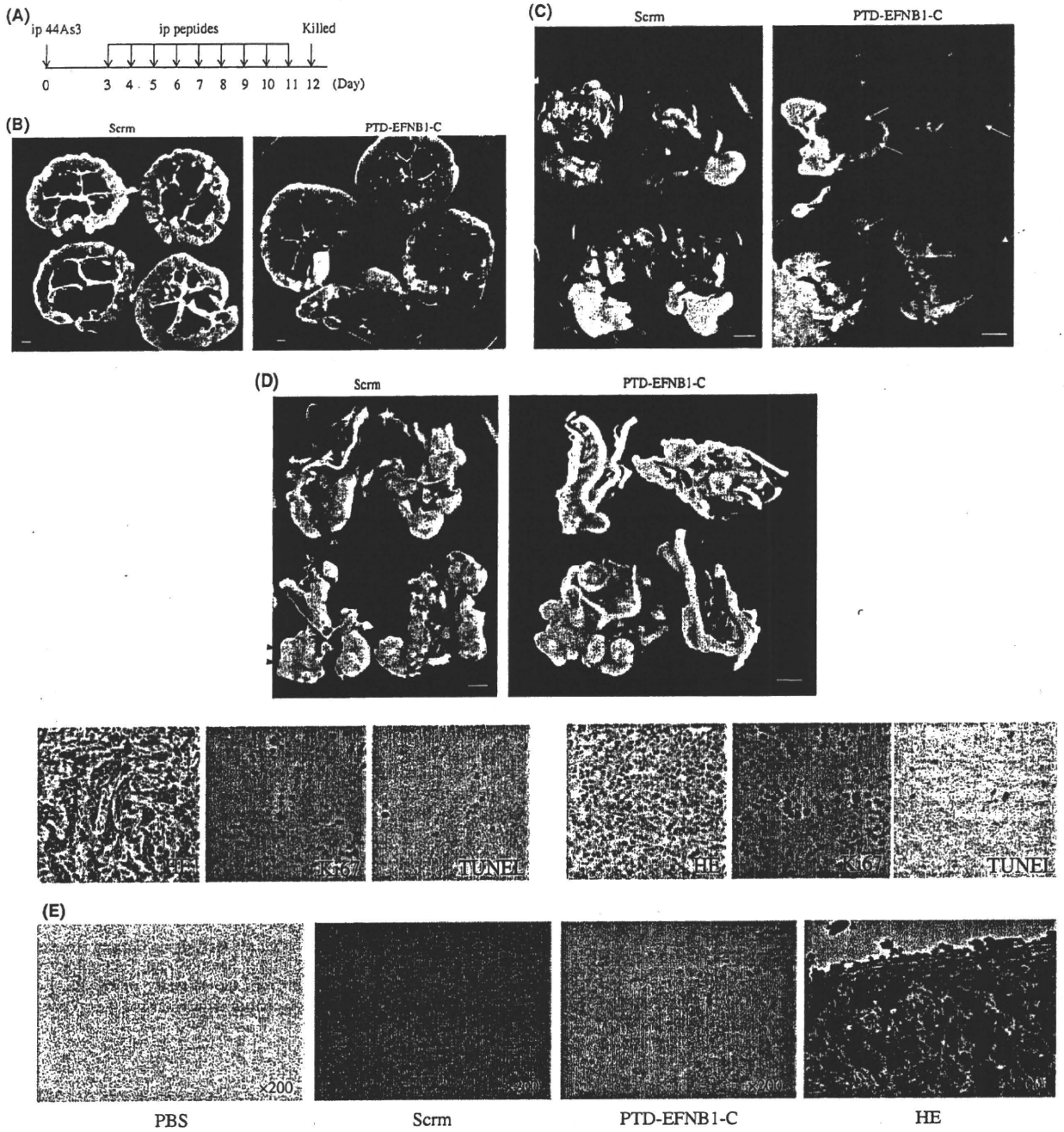

Fig. 4. Fusion protein PTD-EFNB1-C, consisting of the protein transduction domain of HIV-TAT and ephrin-B1$^{331-346}$, inhibits the peritoneal dissemination of scirrhous gastric cancer cells. (A) Time-course schedule of peritoneal dissemination assay. 44As3 scirrhous gastric cancer cells were transplanted in the peritoneal cavity of nude mice (ip). PBS containing control peptide Scrambled (Scrm) or PTD-EFNB1-C was intraperitoneally injected every 24 h after the transplantation of 44As3 cells. Representative appearance of intestinal loops (B) and the paragastric region (C), and tumors involving the rectouterine region (D) were compared. Red arrowheads (C,D) indicate disseminated tumor nodules. Yellow arrows (C) indicate fine tumor nodules in mesentery. In (D), all four mice treated with Scrm, but only one in four mice treated with PTD-EFNB1-C, show clear tumor dissemination. Asterisk indicates the bladder. No significant change was observed in the level of Ki67 and TUNEL staining. (E) Disseminated tumors of nude mice were subjected to immunostaining with anti-TAT antibody to detect the peptides in the tumor tissues. Histology of the tumor is shown at the bottom using H&E staining. PBS, mice treated with PBS without any peptide. Scale bars, 5 mm (B–D). Original magnification, ×200 (D bottom panels, E).

was widely distributed in the tumors *in vivo*, although not in all cells, indicates that the peptide was effectively incorporated into the tumor cells by intraperitoneal injection. It is expected that the tumor suppression effect of PTD-EFNB1-C will be further improved by modification of peptide delivery into tumors. The present study demonstrates the ability of a short peptide derived from the C-terminus of ephrin-B1 to suppress the invasion of cancer cells both *in vitro* and *in vivo*.

Table 1. Intraperitoneal dissemination after i.p. inoculation of cancer cells in mice†

Peptide	No. of nodules in mesentery‡			Paragastric region§	Rectouterine region§	No. of mice survived¶
	0–10	10–30	30+			
PBS	1	2	16	16	17	19
Scrm	1	3	14	16	16	18
PTD-EFNB1-C	12	4	3	3	3	19

†Data are shown as the number of mice bearing a tumor. ‡Number of tumor nodules larger than 2 mm in the mesentery per body. §Number of mice bearing tumor nodules larger than 5 mm. ¶Number of mice survived at 12 days after inoculation of cancer cells.

Table 2. Mean size of tumors in mice injected with a fusion peptide consisting of HIV-TAT and amino acids 331–346 of ephrin-B1 (PTD-EFNB1-C)†

Peptide	Mesentery	*P*	Paragastric region	*P*	Rectouterine region	*P*
PBS	3.2 ± 1.2	NA	7.5 ± 2.0	NA	8.0 ± 2.4	NA
Scrm	3.0 ± 1.1	0.683	6.8 ± 1.7	0.484	7.8 ± 2.1	0.532
PTD-EFNB1-C	1.4 ± 0.6	<0.010	1.8 ± 1.1	<0.001	2.3 ± 1.5	<0.001

†Value for tumor size is given as the mean ± SD (mm). Student's *t*-test was used to compare with PBS-treated group. NA, not applicable; Scrm, Scrambled (control peptide).

PTD-EFNB1-C peptide seems to suppress the dissemination of 44As3 cells in at least two ways. One is blocking the complex formation of ephrin-B1 with Dishevelled, which leads to the suppression of RhoA activation. Inactivation of RhoA and its downstream effector Rock likely suppresses the formation and contraction of stress fiber, thereby attenuating the cell motility. Another mechanism is blocking the MMP-8 secretion accompanied with inactivation of Arf1 GTPase. Because it is not clear which molecules directly mediate ephrin-B1 signaling towards Arf1 activation followed by MMP-8 secretion, we cannot currently conclude whether these two mechanisms are independent or whether they have some cross-talk. In addition, there is evidence that phosphorylation of two tyrosine residues located within the C-terminus of ephrin-B1 (Y343, Y344) affects the interaction with other proteins. For example, interaction of Dishevelled with ephrin-B1 is also regulated by the state of phosphorylation of these two tyrosines.[9] Therefore, we cannot rule out the possibility that PTD-EFNB1-C peptide also modifies signaling depending on the phosphorylation of Y343 and Y344 of ephrin-B1 C-terminus. PTD-EFNB1-C peptide did not directly affect the proliferation of cancer cells, but it may affect the histological appearance of tumors, which influences tumor volume (Fig. 4D). Stromal fibrosis is characteristic for gastric scirrhous carcinomas, and the proliferation of fibrous tissues may promote the growth and invasion of this type of tumor through some cancer–stromal interaction. Treatment of PTD-EFNB1-C peptide suppressed such stromal reaction within the tumors.

Besides the signaling related to the C-terminus of ephrin-B1, ephrin-B1 also induces the signaling through tyrosine phosphorylation of the cytoplasmic domain, which is mainly caused by Src family kinases. We previously reported the suppression of 44As3 peritoneal dissemination by expression of the ephrin-B1 with mutation of four tyrosine residues in the cytoplasmic domain (ephrin-B1 4YF; Y313, 317, 324, and 329), which blocks the signaling mediated by the tyrosine phosphorylation of ephrin-B1.[24] In order to compare the contribution of tyrosine phosphorylation of ephrin-B1 cytoplasmic domain and C-terminus mediated signaling to cancer dissemination, further systematic study will be required comparing the different parts of C-terminal peptides, including tyrosine to phenylalanine mutants. It is also possible that combined therapy by PTD-EFNB1-C used in this study and peptides derived from the aa surrounding the phosphorylated tyrosines of ephrin-B1 cytoplasmic domain might have additional effects for suppressing the promotion of scirrhous gastric carcinoma.

It appears that the peptide therapy targeting ephrin-B1 protein might have a major effect in tumor progression such as tumor invasion, metastasis, and dissemination, rather than in the initiation and proliferation of tumors. Therefore, it is also expected that the effects of the ephrin-B1 peptide on solid tumors would be improved by combination with other treatments including general chemotherapeutic reagents. Our results in this study suggest that the peptide derived from ephrin-B1 C-terminus is a promising model for novel drug design in scirrhous gastric carcinoma and possibly other types of tumors.

Acknowledgments

This work was supported by a Grant-in-Aid for Cancer Research from the Ministry of Education, Culture, Science and Technology of Japan and in part by a Grant-in-Aid from the Ministry of Health, Labor and Welfare of Japan for the third-term Comprehensive Ten-Year Strategy for Cancer Control.

References

1 Murai KK, Pasquale EB. Ephective signaling: forward, reverse and crosstalk. *J Cell Sci* 2003; **116**: 2823–32.
2 Blits-Huizinga C, Nelersa C, Malhotra A, Liebl D. Ephrins and their receptors: binding versus biology. *IUBMB Life* 2004; **56**: 257–65.
3 Poliakov A, Cotrina M, Wilkinson DG. Diverse roles of Eph receptors and ephrins in the regulation of cell migration and tissue assembly. *Dev Cell* 2004; **7**: 465–80.
4 Lin D, Gish GD, Songyang Z, Powson T. The carboxyl terminus of B class ephrins constitutes a PDZ domain binding motif. *J Biol Chem* 1999; **274**: 3726–33.
5 Cowan CA, Henkemeyer M. The SH2/SH3 adaptor Grb4 transduces B-ephrin reverse signals. *Nature* 2001; **413**: 174–9.
6 Bong YS, Park YH, Lee HS, Mood K, Ishimura A, Daar IO. Tyr-298 in ephrin-B1 is critical for an interaction with the Grb4 adaptor protein. *Biochem J* 2004; **377**: 499–507.
7 Tanaka M, Kamo T, Ota S, Sugimura H. Association of dishevelled with Eph tyrosine kinase receptor and ephrin mediates cell repulsion. *The EMBO J* 2003; **22**: 847–58.
8 Lee HS, Bong YS, Moore KB, Soria K, Moody SA, Daar IO. Dishevelled mediates ephrinB1 signalling in the eye field through the planar cell polarity pathway. *Nature Cell Biol* 2005; **8**: 55–63.
9 Lee HS, Mood K, Battu G, Ji YJ, Singh A, Daar IQ. FGF receptor-induced phosphorylation of ephrin-B1 modulates its interaction with Dishevelled. *Mol Boil Cell* 2009; **20**: 124–33.
10 Batlle E, Henderson JT, Beghtel H *et al.* Beta-catenin and TCF mediate cell positioning in the intestinal epithelium by controlling the expression of EphB/ephrinB. *Cell* 2002; **111**: 251–63.
11 Klein R. Eph/ephrin signaling in morphogenesis, neural development and plasticity. *Curr Opin Cell Biol* 2004; **16**: 580–9.
12 Batlle E, Bacani J, Begthel H *et al.* EphB receptor activity suppresses colorectal cancer progression. *Nature* 2005; **435**: 1126–30.
13 Tanaka M, Kamata R, Sakai R. Phosphorylation of ephrin-B1 via the interaction with claudin following cell-cell contact formation. *The EMBO J* 2005; **24**: 3700–11.
14 Holmberg J, Genander M, Halford MM *et al.* EphB receptors coordinate migration and proliferation in the intestinal stem cell niche. *Cell* 2006; **125**: 1151–263.

doi: 10.1111/j.1349-7006.2009.01352.x

15 Meyer S, Hafner C, Guba M *et al.* Ephrin-B2 overexpression enhances integrin-mediated ECM-attachment and migration of B16 melanoma cells. *Int J Oncol* 2005; **27**: 1197–206.
16 Castellvi J, Garcia A, De la Torre J *et al.* EphrinB expression in epithelial ovarian neoplasms correlates with tumor differentiation and angiogenesis. *Hum Pathol* 2006; **37**: 883–9.
17 Kataoka H, Tanaka M, Kanamori M *et al.* Expression profile of EFNB1, EFNB2, two ligands of EPHB2 in human gastric cancer. *J Cancer Res Clin Oncol* 2002; **128**: 343–8.
18 Varelias A, Koblar SA, Cowled PA, Carter CD, Clayer M. Human osteosarcoma express specific ephrin profiles: implications for tumorigenicity and prognosis. *Cancer* 2002; **95**: 862–9.
19 Tanaka M, Sasaki K, Kamata R, Sakai R. The C-terminus of ephrin-B1 regulates metalloproteinase secretion and invasion of cancer cells. *J Cell Sci* 2007; **120**: 2179–89.
20 Siller-Lopez F, Garcia-Banuelos J, Hasty KA *et al.* Truncated active matrix metalloproteinase-8 gene expression in HepG2 cells is active against native type I collagen. *J Hepatol* 2000; **33**: 758–63.
21 Stadlemann S, Pollheimer J, Moser PL *et al.* Cytokine-regulated expression of collagenase-2 (MMP-8) is involved in the progression of ovarian cancer. *Eur J Cancer* 2003; **39**: 2499–505.
22 Lint PV, Libert C. Matrix metalloproteinase-8: cleavage can be decisive. *Cytokine Growth Factor Rev* 2006; **17**: 217–23.
23 Futaki S, Suzuki T, Ohashi W *et al.* Arginine-rich peptides. *J Biol Chem* 2001; **276**: 5836–40.
24 Tanaka M, Kamata R, Takigahira M, Yanagihara K, Sakai R. Phosphorylation of ephrin-B1 regulates dissemination of gastric scirrhous carcinoma. *Am J Pathol* 2007; **171**: 68–78.
25 Tanaka M, Ohashi R, Nakamura R *et al.* Tiam1 mediates neurite outgrowth induced by ephrin-B1 and EphA2. *The EMBO J* 2004; **23**: 1075–88.
26 Yanagihara K, Tanaka H, Takigahira M *et al.* Establishment of two cell lines from human gastric scirrhous carcinoma that possess the potential to metastasize spontaneously in nude mice. *Cancer Sci* 2004; **95**: 575–82.

Cancer Science
The official journal of the Japanese Cancer Association JCA

Phosphatidylinositol 4,5-bisphosphate and PIP5-kinase Iα are required for invadopodia formation in human breast cancer cells

Hideki Yamaguchi,[1,2,3,4] Shuhei Yoshida,[1] Emi Muroi,[1] Masahiro Kawamura,[1] Zen Kouchi,[1] Yoshikazu Nakamura,[1] Ryuichi Sakai[2] and Kiyoko Fukami[1]

[1]Laboratory of Genome and Biosignal, Tokyo University of Pharmacy and Life Sciences, Tokyo; [2]Growth Factor Division, National Cancer Center Research Institute, Tokyo; [3]PRESTO, Japan Science and Technology Agency, Saitama, Japan

(Received February 25, 2010/Revised March 14, 2010/Accepted March 17, 2010/Accepted manuscript online March 24 2010/Article first published online April 23, 2010)

Invadopodia are ventral cell protrusions formed in invasive cancer cells. Because invadopodia have extracellular matrix (ECM) degradation activity, they are thought to function in cancer invasion. In this study, we examined the roles of phosphatidylinositol 4,5-bisphosphate [PI(4,5)P_2] and PI(4,5)P_2-producing enzymes in invadopodia formation in MDA-MB-231 human breast cancer cells. Immunofluorescence analysis showed that PI(4,5)P_2 accumulates at invadopodia on the ventral cell surface. Injection of an anti-PI(4,5)P_2 antibody inhibited invadopodia formation along with gelatin degradation activity. Sequestering of PI(4,5)P_2 by overexpression of the phospholipase C (PLC) δ1-pleckstrin homology (PH) domain, a specific probe for PI(4,5)P_2, also blocked invadopodia formation, while a mutated PLCδ1-PH domain that lacks PI(4,5)P_2-binding activity had no effect. Cellular PI(4,5)P_2 production is mainly mediated by type-I phosphatidylinositol 4-phosphate 5-kinase (PIP5KI) family proteins, which include PIP5KIα, Iβ, and Iγ. Real-time quantitative PCR analysis showed that PIP5KIα is a dominant isoform expressed in MDA-MB-231 cells. Knockdown of PIP5KIα by small-interfering RNA (siRNA) inhibited invadopodia formation and gelatin degradation. Immunofluorescence analysis revealed that endogenous PIP5KIα protein localizes at invadopodia, which is corroborated by the observation that exogenously expressed green fluorescent protein (GFP)-fused PIP5KIα protein also accumulates at gelatin degradation sites. These results indicate that localized production of PI(4,5)P_2 by PIP5KIα is required for invadopodia formation and ECM degradation by human breast cancer cells. (*Cancer Sci* 2010; 101: 1632–1638)

Invadopodia are extracellular matrix (ECM)-degrading protrusions formed at the ventral surface of invasive cancer cells.[1,2] In the case of breast cancer cell lines, the ability to form invadopodia is closely related to their invasive and metastatic properties.[3,4] Additionally, during intravasation, invadopodia-like protrusions in tumor cells have been observed *in vivo* by intravital imaging.[5,6] Therefore, invadopodia are proposed to function in local ECM degradation during cancer invasion and metastasis, although the *in vivo* relevance of invadopodia has yet to be determined. To date, many components of invadopodia have been reported, including proteins involved in the regulation of the actin cytoskeleton, cell signaling, cell–ECM adhesion, ECM degradation, and membrane remodeling.[7–9] We and other researchers previously proposed that invadopodia formation occurs in several steps. Invadopodia precursors are assembled by an actin polymerization machinery containing neural Wiskott–Aldrich syndrome protein (N-WASP), the Arp2/3 complex, and cortactin in response to extracellular stimuli.[3,10] The invadopodia precursors are then stabilized by further actin polymerization induced by cofilin and Mena, and finally these structures gather matrix metalloproteinases to mature into functional invadopodia.[3,11,12] However, it is unknown how these events occur at the restricted sites on the plasma membrane of invasive cancer cells.

The membrane phospholipid phosphatidylinositol 4,5-bisphosphate [PI(4,5)P_2] regulates diverse cellular processes, including signal transduction, endocytosis/phagocytosis, vesicular trafficking, and actin cytoskeletal reorganization.[13] PI(4,5)P_2 acts as a substrate for phospholipase C (PLC) and phosphatidylinositol 3-kinase (PI3K), while it also directly regulates the activity and localization of target proteins that have a PI(4,5)P_2 binding domain.[14] PI(4,5)P_2 production in mammalian cells is primarily mediated by type I phosphatidylinositol 4-phosphate 5-kinase (PIP5KI), which phosphorylates phosphatidylinositol 4-phosphate at the D-5 position of the inositol ring.[15] Three isoforms of PIP5KI (PIP5KIα, Iβ, and Iγ in human nomenclature) and two alternatively spliced isoforms of PIP5KIγ (Iγ635 and Iγ661) have been identified in mammalian cells.[16] Because the subcellular localization of PIP5KIs is unique to each isoform, they seem to have distinct cellular functions.[17,18]

Previous reports have identified that the localization and activity of several invadopodia components, such as N-WASP, cofilin, and dynamin-2, are regulated by PI(4,5)P_2 [19,20] Additionally, Arf6, an essential regulator of invadopodia formation,[21,22] is known to activate PIP5KIs and, therefore, stimulate PI(4,5)P_2 synthesis.[23] However, the importance of PI(4,5)P_2 and PIP5KIs in invadopodia formation is yet to be determined.

Here, we studied the roles of PI(4,5)P_2 and PIP5KIs in invadopodia formation. We found that PI(4,5)P_2 and PIP5KIα are essential regulators of invadopodia-mediated ECM degradation by human breast cancer cells.

Materials and Methods

Cell culture. MDA-MB-231 human breast cancer cell line was obtained from the American Type Culture Collection (Manassas, VA, USA) and cultured as described previously.[4]

Antibodies, reagents, and constructs. Alexa dyes, fluorescence-labeled phalloidin, and secondary antibodies were purchased from Invitrogen (Carlsbad, CA, USA). Gelatin and other chemicals were purchased from Sigma (St. Louis, MO, USA). Anti-PI(4,5)P_2 antibody has been described previously.[24] Anti-PIP5KIα and anti-β-actin antibodies were purchased from Santa Cruz Biotechnology (Santa Cruz, CA, USA) and Millipore (Billerica, MA, USA), respectively. Anti-Akt and anti-phospho-Akt (Ser473) antibodies were purchased from Cell Signaling Technology (Danvers, MA, USA). Green fluorescent protein (GFP)-PIP5KIα constructs were kindly provided by Dr Kanaho

[4]To whom correspondence should be addressed. E-mail: hidyamag@ncc.go.jp

doi: 10.1111/j.1349-7006.2010.01574.x

(Tsukuba University, Ibaraki, Japan). For GFP-PLCδ1-pleckstrin homology (PH) domain constructs, cDNA encoding the mouse PLCδ1-PH domain (amino acid 1–140) was subcloned into pEGFP-C1 vector (Clontech, Mountain View, CA, USA). A PrimeSTAR Mutagenesis Basal Kit (Takara Bio, Shiga, Japan) was used to generate the R40D mutant of the PLCδ1-PH domain.

Plasmid transfection. Cells were transfected with the indicated plasmids using Lipofectamine LTX (Invitrogen) according to the manufacturer's instructions.

RNA interference. Stealth RNAi (Invitrogen) molecules were used for RNA interference (RNAi) experiments: Negative Control Medium GC Duplex #2, Stealth Select RNAi for PIP5KIα (HSS144742 and HSS144743) and for PIP5KIγ (HSS118703). Cells were transfected with 30 nM small-interfering RNA (siRNA) using Lipofectamine RNAiMAX (Invitrogen) according to the manufacturer's instructions. The cells were cultured for 48–72 h and subjected to invadopodia assay, reverse transcriptase–polymerase chain reaction (RT-PCR) analysis, or immunoblotting.

RT-PCR. Standard PCR amplification was performed as described previously.[4] The sequences of primer pairs used were as follows: human cyclophilin B2 (5′-GCACAGGAGGAAAGAGCATC-3′ and 5′-CTTCTCCACCTCGATCTTGC-3′), human PIPK Iα (5′-TGCCCATCAAGAAAATAGGC-3′ and 5′-GAAGTAGCGGAAGGCAACAG-3′), human PIPK Iβ (5′-AGACACAATGGGAGGCATTC-3′ and 5′-TCTCCTGTGAAGTGGCCTTT-3′), and human PIPK Iγ (5′-CAGGACTTCCGCTTCAAGAC-3′ and 5′-CACGCAGTACAGCCCATAGA-3′). Quantitative RT-PCR was performed with Thunderbird qPCR Mix (Toyobo, Osaka, Japan) in a CFX96 Real-Time PCR Detection System (Bio-Rad Laboratories, Hercules, CA, USA). The primer pairs used were as follows: human cyclophilin B2 (5′-TTCTAGAGGGCATGGAGGTG-3′ and 5′-GCTTCTCCACCTCGATCTTG-3′), human PIPK Iα (5′-CGGTCTGGCTCATCTTTCTC-3′ and 5′-AAACATCAGGACGACCAAGG-3′), human PIPK Iβ (5′-AAGGATGAGAAGCGGGATTT-3′ and 5′-AATTGTGGTTGCCAAGGAAG-3′), and human PIPK Iγ (5′-AGAAGCCACTACAGCCTCCA-3′ and 5′-CCTGTCCAGACGACTGTGTG-3′). These primer pairs have almost the same amplification efficiencies. Human mosaic cDNA template (Toyobo) was used as a positive control.

Epidermal growth factor (EGF) stimulation and immunoblotting. Cells were serum-starved overnight in 0.35% bovine serum albumin/medium and stimulated with 50 ng/mL EGF for 10 min at 37°C. The cells were then lysed in lysis buffer containing 50 mM Tris–HCl, pH 7.5, 1% NP-40, 2 mM EDTA, 100 mM NaCl, 1 mM sodium orthovanadate, and a protease inhibitor cocktail (Roche, Basel, Switzerland). The lysates were subjected to immunoblot analysis as described previously.[3] To quantify the phospho-Akt amount, densitometry was performed on scanned immunoblot images using the ImageJ 1.410 (National Institutes of Health, Bethesda, Maryland, USA, http://rsbwep.nih.gov/ij/) gel analysis tool.

Immunofluorescence. Cells were stained with indicated antibodies and phalloidins as described previously.[3] $PI(4,5)P_2$ staining was also performed as described.[25] Samples were observed with an Olympus IX81-ZDC-DSU confocal microscope (Olympus, Tokyo, Japan) equipped with a cooled charged-coupled device (CCD) camera (ORCA-ER: Hamamatsu, Shizuoka, Japan). Images were analyzed and processed with Metamorph (Universal Imaging, Buckinghamshire, UK), ImageJ 1.41o, and Adobe Photoshop software.

Invadopodia assay. Fluorescent gelatin-coated dishes were prepared as described previously.[26] In brief, gelatin was labeled with TRITC in borate buffer (40 mM NaCl, 50 mM $Na_2B_4O_7$, pH 9.3) and extensively dialyzed against phosphate-buffered saline (PBS). Coverslips (12 mm, circular) were coated with 25 mg/mL fluorescent gelatin and 20 mg/mL sucrose in PBS, and then crosslinked with 0.5% glutaraldehyde on ice for 15 min followed by 30 min at room temperature. After extensive washing with PBS, the coverslips were treated with 5 mg/mL sodium borohydrate for 3 min to quench autofluorescence of residual glutaraldehyde. The coverslips were then sterilized with 70% ethanol for 15 min and quenched in growth medium for 1 h before plating cells. Cells were cultured on the gelatin matrix for 3–7 h and then stained with the appropriate antibody and phalloidin to visualize invadopodia and gelatin degradation sites. To quantitate the degradation activity of invadopodia, the degradation area was calculated from images using ImageJ 1.41o software and normalized for the number of cells. In the cases of antibody microinjection and GFP-PLCδ1 PH domain overexpression, the average values of control cells were set to 100% and relative degradation activities were shown. Data were obtained from three independent experiments. For siRNA knockdown experiments, at least 40 transfected cells were analyzed for each sample and the values of control cells were set to 100% in each experiment. Data shown are mean ± SE of four independent experiments.

Antibody microinjection. Cells were plated onto fluorescent gelatin, cultured for 2 h, and then microinjected with anti-$PI(4,5)P_2$ antibody or control mouse immunoglobulin G (IgG) using a microinjection system (Eppendorf, Hamburg, Germany). The cells were further cultured for 3 h to allow them to form invadopodia and degrade the gelatin matrix. Cells were then fixed and stained with Alexa Fluor 488-conjugated antimouse IgG antibody and Alexa Fluor 633-phalloidin to detect microinjected cells and invadopodia, respectively.

Quantification of the cellular $PI(4,5)P_2$ amount. A $PI(4,5)P_2$ Mass ELISA Kit (Echelon Biosciences, Salt Lake City, UT,

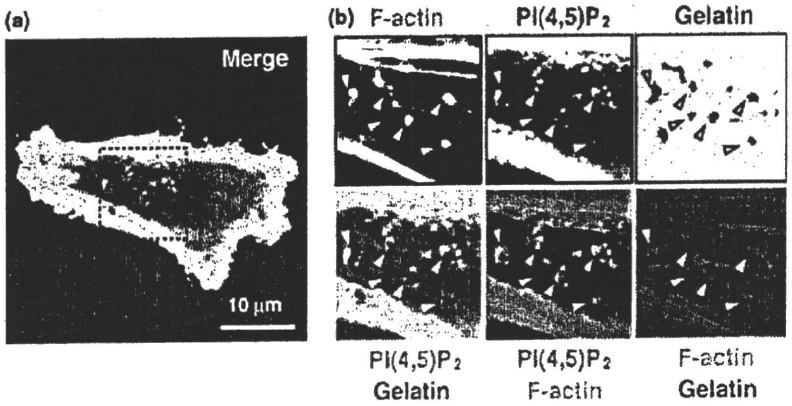

Fig. 1. $PI(4,5)P_2$ accumulates at invadopodia formed in human breast cancer cells. (a) MDA-MB-231 cells were cultured on coverslips coated with fluorescent gelatin (red) and stained with anti-$PI(4,5)P_2$ antibody (green) and phalloidin (blue) as described in the Materials and Methods. Right panels are magnified images of the boxed region. Arrowheads denote accumulation of $PI(4,5)P_2$ signals at invadopodia.